

# Functional and Highly Crosslinkable HIV-1 Envelope Glycoproteins Enriched in a Pretriggered Conformation

Hanh T. Nguyen<sup>a,b,\*</sup>, Alessandra Qualizza<sup>a</sup>, Saumya Anang<sup>a,b</sup>, Meiqing Zhao<sup>a</sup>, Shitao Zou<sup>a</sup>, Rong Zhou<sup>a</sup>, Qian Wang<sup>a,b</sup>, Shijian Zhang<sup>a,b</sup>, Ashlesha Deshpande<sup>c,d</sup>, Haitao Ding<sup>c,d</sup>, Amos B. Smith III<sup>e</sup>, John C. Kappes<sup>c,d</sup> and Joseph G. Sodroski<sup>a,b,\*</sup>

<sup>a</sup>Department of Cancer Immunology and Virology, Dana-Farber Cancer Institute, Boston, MA 02215, USA

<sup>b</sup>Department of Microbiology, Harvard Medical School, Boston, MA 02215, USA

<sup>c</sup>Department of Medicine, University of Alabama at Birmingham, AL 35294, USA

<sup>d</sup>Birmingham Veterans Affairs Medical Center, Research Service, Birmingham, AL 35233, USA

<sup>e</sup>Department of Chemistry, University of Pennsylvania, Philadelphia, Pennsylvania 19104 USA

\*Corresponding authors:

22 Hanh T. Nguyen, Ph.D.

23 Joseph G. Sodroski, M.D.

24 Dana-Farber Cancer Institute

25 450 Brookline Avenue, CLS 1010

26 Boston, MA 02215

27 Phone: 617-632-3371 Fax: 617-632-4338

Email: hanh.nguyen@dfci.harvard.edu; joseph.sodroski@dfci.harvard.edu

30 Running title: Crosslinkable HIV-1 Envs enriched in State 1

31

32 Word count for the Abstract: 250

33

34 **ABSTRACT**

35 Binding to the receptor, CD4, drives the pretriggered, “closed” (State-1) conformation of  
36 the human immunodeficiency virus (HIV-1) envelope glycoprotein (Env) trimer into more  
37 “open” conformations (States 2 and 3). Broadly neutralizing antibodies, which are  
38 elicited inefficiently, mostly recognize the State-1 Env conformation, whereas the more  
39 commonly elicited poorly neutralizing antibodies recognize States 2/3. HIV-1 Env  
40 metastability has created challenges for defining the State-1 structure and developing  
41 immunogens mimicking this labile conformation. The availability of functional State-1  
42 Envs that can be efficiently crosslinked at lysine and/or acidic amino acid residues might  
43 assist these endeavors. To that end, we modified HIV-1<sub>AD8</sub> Env, which exhibits an  
44 intermediate level of triggerability by CD4. We introduced lysine/acidic residues at  
45 positions that exhibit such polymorphisms in natural HIV-1 strains. Env changes that  
46 were tolerated with respect to gp120-gp41 processing, subunit association and virus  
47 entry were further combined. Two common polymorphisms, Q114E and Q567K, as well  
48 as a known variant, A582T, additively rendered pseudoviruses resistant to cold, soluble  
49 CD4 and a CD4-mimetic compound, phenotypes indicative of stabilization of the  
50 pretriggered State-1 Env conformation. Combining these changes resulted in two  
51 lysine-rich HIV-1<sub>AD8</sub> Env variants (E.2 and AE.2) with neutralization- and cold-resistant  
52 phenotypes comparable to those of natural, less triggerable Tier 2/3 HIV-1 isolates.  
53 Compared with these and the parental Envs, the E.2 and AE.2 Envs were cleaved more  
54 efficiently and exhibited stronger gp120-trimer association in detergent lysates. These  
55 highly crosslinkable Envs enriched in a pretriggered conformation should assist  
56 characterization of the structure and immunogenicity of this labile state.

57 **IMPORTANCE**

58 The development of an efficient vaccine is critical for combating HIV-1 infection  
59 worldwide. However, the instability of the pretriggered shape (State 1) of the viral  
60 envelope glycoprotein (Env) makes it difficult to raise neutralizing antibodies against  
61 HIV-1. Here, by introducing multiple changes in Env, we derived two HIV-1 Env  
62 variants that are enriched in State 1 and can be efficiently crosslinked to maintain this  
63 shape. These Env complexes are more stable in detergent, assisting their purification.  
64 Thus, our study provides a path to a better characterization of the native pretriggered  
65 Env, which should assist vaccine development.

66

67 **KEYWORDS:** human immunodeficiency virus, envelope, polymorphism, native  
68 conformation, state 1, stabilizing mutation, chemical crosslink

69

70

71 **INTRODUCTION**

72 Human immunodeficiency virus type 1 (HIV-1) entry into target cells is mediated by the  
73 viral envelope glycoprotein (Env) trimer (1,2). The Env trimer is composed of three  
74 gp120 exterior subunits and three gp41 transmembrane subunits (2). In infected cells,  
75 Env is first synthesized as an uncleaved precursor in the rough endoplasmic reticulum  
76 (ER), where signal peptide cleavage, folding, trimerization, and the addition of high-  
77 mannose glycans take place (3-6). Exiting the ER, the trimeric gp160 Env precursor  
78 follows two pathways to the cell surface (7). In the conventional secretory pathway, the  
79 Env precursor transits through the Golgi compartment, where it is cleaved into gp120  
80 and gp41 subunits and is further modified by the addition of complex sugars. These  
81 mature Envs are transported to the cell surface and are incorporated into virions (8-11).  
82 In the second pathway, the gp160 precursor bypasses processing in the Golgi and  
83 traffics directly to the cell surface; these Golgi-bypassed gp160 Envs are excluded from  
84 virions (7).

85

86 Single-molecule fluorescence resonance energy transfer (smFRET) experiments  
87 indicate that, on virus particles, the mature (cleaved) Env trimer exists in three  
88 conformational states (States 1-3) (12). From its pretriggered conformation (State 1),  
89 the metastable Env trimer interacts with the receptors, CD4 and CCR5 or CXCR4, and  
90 undergoes transitions to lower-energy states (2, 12-23). Initially, the engagement with  
91 CD4 induces an asymmetric intermediate Env conformation (State 2) (24, 25). Binding  
92 of additional CD4 molecules to the Env trimer then induces the full CD4-bound,  
93 prehairpin intermediate conformation (State 3) (24-31). An extended coiled coil  
94 consisting of the heptad repeat (HR1) region of gp41 is exposed in the prehairpin

95 intermediate (23, 25, 29-31). State 3 Env subsequently interacts with the CCR5 or  
96 CXCR4 coreceptor to trigger the formation of a gp41 six-helix bundle, a process that  
97 results in fusion of the viral and target cell membranes (32-36).

98

99 Env strain variability, heavy glycosylation and conformational flexibility contribute  
100 to HIV-1 persistence by avoiding the binding of potentially neutralizing antibodies.  
101 Mature Envs from primary HIV-1 strains largely reside in a State-1 conformation, which  
102 resists the binding of most antibodies elicited during natural infection (12, 23, 37-39);  
103 these high-titer, poorly neutralizing antibodies often recognize State-2/3 Env  
104 conformations (40-44). After years of infection, a small percentage of HIV-1-infected  
105 individuals generate broadly neutralizing antibodies (bNAbs), most of which recognize  
106 the State-1 Env conformation (12, 37, 38, 45-54). Passively administered monoclonal  
107 bNAbs have been shown to be protective in animal models of HIV-1 infection,  
108 suggesting that the elicitation of bNAbs is an important goal for vaccines (55-60).  
109 Unfortunately, bNAbs have not been efficiently and consistently elicited in animals  
110 immunized with current HIV-1 vaccine candidates, including stabilized soluble gp140  
111 (sgp140) SOSIP.664 trimers (61-69). Compared with functional membrane Envs,  
112 differences in the antigenicity, glycosylation and conformation of sgp140 SOSIP.664  
113 trimers have been observed (70-77), potentially contributing to the inefficiency of bNAb  
114 elicitation. Single-molecule FRET (smFRET) analysis indicates that the sgp140  
115 SOSIP.664 trimers assume a State-2-like conformation (78). These studies imply that  
116 the available structures of sgp140 SOSIP.664 and other detergent-solubilized Env  
117 trimer preparations (27, 28, 77, 79-91) differ from that of State-1 Env. The extent of the  
118 structural differences between the State-1 and State-2 Env conformations and their

119 potential impact on Env immunogenicity are unknown. However, the importance of the  
120 State-1 Env as a likely target of vaccine-induced bNAbs provides a rationale for better  
121 characterization of this conformation.

122

123 HIV-1 is a polymorphic virus with a high mutation rate, allowing escape from host  
124 immune responses and antiretroviral drugs (92-99). Env polymorphisms that arise  
125 naturally or as a result of tissue-culture adaptation can result in altered virus infectivity,  
126 receptor binding or neutralization sensitivity (23, 40, 44-46, 100-119). Specifically,  
127 changes in “restraining residues” in gp120 have been shown to destabilize State 1,  
128 disrupt the closed pretriggered Env conformation, and lead to increased sampling of  
129 downstream conformations (45, 118, 119). These more “triggerable” Env mutants  
130 exhibit increased sensitivity to cold, soluble CD4 (sCD4), CD4-mimetic compounds and  
131 poorly neutralizing antibodies (23, 37, 45, 118, 119). Less common Env alterations  
132 apparently decrease Env triggerability and stabilize a State-1 conformation (120-125).

133

134 Crosslinking of HIV-1 Env amino acid residues, in some cases combined with  
135 mass spectrometry, has been used to study Env conformations (37, 73, 126-131).  
136 Crosslinking protocols that target lysine or acidic amino acid residues on native proteins  
137 have been integrated with mass spectrometry to provide low-resolution structural  
138 information (132-135). Here, we introduced lysine and acidic amino acid residues into a  
139 primary HIV-1 Env, using natural polymorphisms as a guide. Env changes that were  
140 functionally tolerated were combined to create Envs that are potentially able to be  
141 conformationally fixed by treatment with specific crosslinking agents. In the process of  
142 generating these Env variants, we identified two common polymorphisms that increased

143 virus resistance to cold, sCD4 and a CD4-mimetic compound, phenotypes associated  
144 with stabilization of a pretriggered (State-1) Env conformation (120-125). Two lysine-  
145 rich variants with cold- and sCD4-resistant phenotypes were cleaved more efficiently  
146 and exhibited stronger gp120-trimer association in detergent lysates compared with the  
147 parental HIV-1 Env. Such highly crosslinkable Envs enriched in a pretriggered  
148 conformation should assist characterization of State 1.

149

## 150 **RESULTS**

### 151 **Env variants with common lysine and acidic residue polymorphisms**

152 We sought to create functional primary HIV-1 Env variants with an increased number of  
153 lysine/acidic residues that could be used to introduce stabilizing crosslinks. To identify  
154 Env residues that might potentially tolerate such substitutions, we compared Env  
155 sequences from 193 Group M, N, O and P HIV-1 and SIV<sub>cpz</sub> strains (136). We identified  
156 Env residues where lysine or acidic substitutions occurred in at least 5% of these  
157 natural virus strains from more than one phylogenetic clade. The lysine polymorphisms  
158 were grouped by location in Env regions (gp41 and gp120 C-terminus, gp120 trimer  
159 association domain and gp120 inner domain) and by the number of substitutions in a  
160 set (Sets 4-7 contain additional lysine substitutions compared with those in Sets 1-3)  
161 (Fig. 1A). The ED2 set contains seven of the most common aspartic acid and glutamic  
162 acid polymorphisms in natural HIV-1/SIV<sub>cpz</sub> variants (Fig. 1A).

163

164 We selected the primary Clade B HIV-1<sub>AD8</sub> as the source of the parental “wild-  
165 type” Env in this study. Primary HIV-1 Envs differ in triggerability by CD4, a property  
166 that influences virus resistance to sCD4, CD4-mimetic compounds and some antibodies

167 (23). The HIV-1<sub>AD8</sub> Env is efficiently expressed and processed, is well characterized  
168 with respect to antibody binding and neutralization sensitivity (Tier 2) and, among  
169 primary HIV-1 Envs, exhibits an intermediate level of triggerability by CD4 (7, 23, 73).  
170 Single, double and triple sets of lysine substitutions were introduced into the wild-type  
171 HIV-1<sub>AD8</sub> Env. For example, double sets included Sets 1 + 2, 1 + 3, 2 + 3, 2 + 4, 3 + 5,  
172 etc.; triple sets included Sets 1 + 2 + 3, 2 + 3 + 4, 2 + 3 + 6, 3 + 6 + 7, etc. (Fig. 1A). In  
173 a preliminary study, a total of 24 Env variants were analyzed for protein expression and  
174 processing, ability to support entry of a pseudotyped virus, and the sensitivity of the viral  
175 pseudotype to neutralization by the 19b antibody. The 19b antibody is a poorly  
176 neutralizing antibody that recognizes the gp120 V3 loop and serves as a sensitive  
177 indicator of HIV-1 Env transitions to State-2/3 conformations (45, 71-74, 137). With a  
178 few exceptions, most of the lysine substitutions were well tolerated with respect to HIV-  
179 1<sub>AD8</sub> Env processing, virus infectivity and sensitivity to 19b neutralization (data not  
180 shown). However, Envs with Set 3 + 7 and Set 3 + 6 +7 changes were poorly  
181 processed and inefficiently supported pseudovirus infection. Viruses with Set 3 + 5  
182 changes were more sensitive than the wild-type HIV-1<sub>AD8</sub> to neutralization by the 19b  
183 antibody (data not shown). Thus, while most of the introduced lysine substitutions were  
184 well tolerated, some specific combinations apparently exert undesirable effects on HIV-  
185 1<sub>AD8</sub> Env conformation and function.

186

### 187 **Lysine-rich 2-4 R and 2-4 RED2 Envs**

188 Based on the results of our preliminary analysis, we selected the 2-4 R Env, which  
189 contains Set 2 + 4 and R315K changes, for more detailed characterization. The ED2  
190 set of acidic substitutions was also added to the 2-4 R Env to create the 2-4 RED2 Env

191 (Fig. 1B). Both 2-4 R and 2-4 RED2 Envs mediated pseudovirus infection as efficiently  
192 as the wild-type HIV-1<sub>AD8</sub> Env (data not shown). To evaluate Env expression,  
193 proteolytic processing and gp120-trimer association, HOS cells were transfected with  
194 plasmids expressing the wild-type HIV-1<sub>AD8</sub> Env and the 2-4 R and 2-4 RED2 Envs  
195 tagged at the C-terminus with His<sub>6</sub>. Cell lysates were Western blotted directly (Input) or  
196 were precipitated with nickel-nitrilotriacetic (Ni-NTA) beads in the presence of BMS-806,  
197 sCD4 or the DMSO control. BMS-806 is a small-molecule HIV-1 entry inhibitor that  
198 binds gp120 and stabilizes a State-1-like Env conformation (12, 78, 138-140). The  
199 uncleaved gp160 Env precursor and mature gp120 and gp41 glycoproteins were  
200 detected in lysates of cells expressing the wild-type HIV-1<sub>AD8</sub>, 2-4 R and 2-4 RED2 Envs  
201 (Fig. 2A). Comparison of the gp120:gp160 ratio in the cell lysates indicates that the 2-4  
202 R and 2-4 RED2 Envs are processed more efficiently than the wild-type HIV-1<sub>AD8</sub> Env  
203 (Fig. 2A, Input lanes). In the DMSO control sample, although wild-type HIV-1<sub>AD8</sub> gp41  
204 and gp160 were precipitated by the Ni-NTA beads, little gp120 was coprecipitated (Fig.  
205 2A, Ni-NTA lanes). Apparently, under these conditions, gp120 dissociates from the  
206 wild-type HIV-1<sub>AD8</sub> Env complex. BMS-806 increased the association of the wild-type  
207 HIV-1<sub>AD8</sub> gp120 with the precipitated Env complex, as previously seen (138). In the  
208 presence of sCD4, no coprecipitated gp120 was detected, presumably as a result of  
209 CD4-induced gp120 shedding (141, 142). Compared with the wild-type HIV-1<sub>AD8</sub> Env,  
210 the 2-4 R gp120 was precipitated more efficiently by the Ni-NTA beads in the DMSO  
211 control lysates. The coprecipitation of the 2-4 RED2 gp120 from the DMSO-treated cell  
212 lysates by the Ni-NTA beads was even more efficient. For both 2-4 R and 2-4 RED2  
213 Envs, the association of gp120 with the Env complex was enhanced by BMS-806 and  
214 decreased by sCD4. Thus, the Env changes in 2-4 R and 2-4 RED2 can enhance Env

215 processing and, in detergent lysates, strengthen the association of gp120 with  
216 solubilized Env trimers. Both phenotypes were more pronounced for the 2-4 RED2 Env  
217 than for the 2-4 R Env.

218

219 The sensitivity of viruses with the wild-type HIV-1<sub>AD8</sub>, 2-4 R and 2-4 RED2 Envs  
220 to neutralization by broadly and poorly neutralizing antibodies was examined. The  
221 broadly neutralizing antibodies (bNAbs) in our panel included VRC01 and VRC03  
222 against the CD4-binding site of gp120 (143, 144), PG16 against a quaternary V2  
223 epitope (145), PGT121 against a V3-glycan epitope on gp120 (146), and 35O22 against  
224 the gp120-gp41 interface (147). The poorly neutralizing antibodies included 17b against  
225 a CD4-induced epitope (148), 19b against the gp120 V3 loop (137), 902090 against a  
226 V2 gp120 epitope (149) and F105 against the CD4-binding site of gp120 (150). The 2-4  
227 R and 2-4 RED2 viruses were neutralized by bNAbs comparably to the wild-type HIV-  
228 1<sub>AD8</sub>; like the wild-type HIV-1<sub>AD8</sub>, the 2-4 R and 2-4 RED2 viruses were resistant to  
229 poorly neutralizing antibodies (Fig. 2B).

230

231 The sensitivity of HIV-1 to inactivation by exposure to cold, sCD4 or CD4-mimetic  
232 compounds can provide an indication of Env “triggerability,” the tendency to make  
233 transitions from State 1 (23, 37, 45, 118, 120-125). Compared with the wild-type  
234 HIV-1<sub>AD8</sub>, the 2-4 R virus displayed slight but reproducible resistance to cold, sCD4 and  
235 BNM-III-170, a CD4-mimetic compound (151) (Fig. 2C). The 2-4 RED2 virus exhibited  
236 an even higher level of resistance to cold, sCD4 and BNM-III-170 than either the wild-  
237 type or the 2-4 R virus. These phenotypes are consistent with the stability of the State-

238 1 Env conformation exhibiting the following rank order in these variants: 2-4 RED2 > 2-4  
239 R > wild-type HIV-1<sub>AD8</sub>.

240

## 241 **Q114E and Q576K changes determine State 1-stabilizing phenotypes**

242 We wished to identify the changes in 2-4 RED2 and 2-4 R responsible for the above  
243 phenotypes. Because differences among the wild-type HIV-1<sub>AD8</sub>, 2-4 R and 2-4 RED2  
244 Envs were most apparent in the Ni-NTA coprecipitation and virus sensitivity  
245 experiments, we used these assays to characterize HIV-1<sub>AD8</sub> Env mutants with single-  
246 residue changes corresponding to those in the 2-4 R and 2-4 RED2 Envs. Among the  
247 acidic residue substitutions found in the ED2 set, a single change, Q114E, was  
248 sufficient to recapitulate the 2-4 RED2 Env phenotypes (Fig. 3A). Similarly, a single  
249 lysine substitution originally found in Set 4, Q576K, was responsible for most of the 2-4  
250 R Env phenotypes (Fig. 3B). Thus, Q114E or Q567K alone can enhance HIV-1<sub>AD8</sub> Env  
251 processing, gp120-trimer association and virus resistance to cold, sCD4 and a CD4-  
252 mimetic compound.

253

254 Gln 114 is located in the gp120  $\alpha$ 1 helix, part of the gp120 inner domain that  
255 faces the trimer axis and interacts with gp41 (79-82, 152-155). Gln 567 resides in the  
256 N-terminal segment of the gp41 heptad repeat 1 (HR1<sub>N</sub>) region, which participates in  
257 the formation of the gp41 coiled coil after CD4 binding (32-34). In the available Env  
258 trimer structures, which have been suggested to represent a State-2-like conformation  
259 (78), the HR1<sub>N</sub> region is disordered or structurally heterogeneous (79-89). Although  
260 structural information on Gln 114 and Gln 567 in the context of a State-1 Env is  
261 currently unavailable, based on their approximate location near the trimer axis and the

262 charge complementarity of the substitutions yielding similar phenotypes, we tested their  
263 functional dependence. The phenotypes of a panel of 18 single and double Q114/Q567  
264 Env variants were characterized (Table 1). Only acidic residue substitutions at position  
265 114 resulted in an improvement of the constellation of State-1-associated phenotypes.  
266 At position 567, lysine substitution yielded the strongest State-1-associated phenotypes,  
267 while arginine substitution exerted a more modest effect. Analysis of the double  
268 mutants yielded two insights. First, the phenotypes of the Q114E mutant were not  
269 significantly affected by changing Gln 567 to an alanine residue. Likewise, the  
270 phenotypes of the Q567K mutant were similar to those of the Q567K/Q114A double  
271 mutant. Therefore, the State-1-associated phenotypes of the Q114E and Q567K  
272 mutants are not dependent on the formation of hydrogen bonds between the side  
273 chains of residues 114 and 567. Second, the phenotypic effects of the changes in  
274 residues 114 and 567 were additive. Combination of the strongest individual changes  
275 yielded the variant, Q114E/Q567K, with the most pronounced phenotype. Both  
276 changes are found in the 2-4 RED2 Env. In summary, the Q114E and Q567K changes  
277 independently impart their individual effects on Env function and these effects are  
278 additive.

279

280 We extended our mutagenesis approach to evaluate the potential of other Env  
281 residues to influence the Q114E and Q567K phenotypes. A State-1 Env structure  
282 would be most relevant to the search for interacting partners, but is currently not  
283 available. Therefore, we used the available structural models, many of which represent  
284 State-2-like Env conformations (78), to suggest candidate amino acid residues. In  
285 sgp140 SOSIP.664 trimers, the highly conserved His 72 is located ~8 Å from Gln 114

286 (79-81). Replacing His 72 with lysine or glutamine residues resulted in increased  
287 sensitivity to sCD4 and BNM-III-170; these phenotypes were partially relieved when  
288 these His 72 changes were combined with Q114E (Table 2). Replacing His 72 with an  
289 alanine residue resulted in a virus with neutralization sensitivity similar to that of the  
290 wild-type virus. Compared with the Q114E virus, the H72A/Q114E virus was less  
291 resistant to cold and sCD4. Thus, some changes in His 72 result in an apparent  
292 increase in Env triggerability and can influence the Q114E phenotypes.

293

294 In HIV-1/SIV<sub>cpz</sub> Envs, Thr/Lys polymorphism in residue 202 often exhibits  
295 covariance with Gln/Glu polymorphism in residue 114 (136). Compared with the wild-  
296 type HIV-1<sub>AD8</sub>, viruses with Thr 202 replaced by alanine, lysine, arginine or glutamine  
297 residues were more sensitive to cold, BNM-III-170 and the 19b anti-V3 antibody (Table  
298 2 and data not shown). These phenotypes, which are indicative of increased Env  
299 triggerability and State 1 destabilization, were minimally compensated by the addition of  
300 the Q114E change. Replacing the conserved Gln 203 residue with an alanine residue  
301 (Q203A in Table 2) also resulted in a State-1-destabilized phenotype, but in this case,  
302 the Q114E/Q203A mutant exhibited phenotypes close to that of the wild-type HIV-1<sub>AD8</sub>.  
303 Thus, the Q114E change can compensate for some but not all State 1-destabilizing  
304 changes.

305

306 In the unliganded sgp140 SOSIP.664 and PGT151-bound EnvΔCT structures  
307 (PDB: 4ZMJ and 5 FUU, respectively) (82,86), the side chains of Gln 114, Lys 117 and  
308 Lys 121 from each Env protomer point towards the trimer axis, stacking in three layers.  
309 Interprotomer Lys 117-Lys 117 and Lys 121-Lys 121 crosslinks were formed in a

310 crosslinking/mass spectrometry study of the sgp140 SOSIP.664 trimer, confirming the  
311 location of these residues in the trimer core in these Env structures (73). Substitution of  
312 Lys 117 or Lys 121 with an alanine or glutamine residue resulted in viruses that were  
313 more resistant to cold and BNM-III-170 than the wild-type virus (Table 2). No additive or  
314 synergistic effect was observed when the Q114E change was combined with the K117A  
315 or K121A changes. In fact, the double mutants exhibited less stable association of  
316 gp120 with solubilized Env trimers (Table 2). Thus, the effects of the Gln 114, Lys 117  
317 and Lys 121 changes on the viral phenotypes are redundant, whereas in the detergent-  
318 solubilized Envs, the K117A and K121A changes nullify the trimer-stabilizing effects of  
319 the Q114E change. Similar phenotypic effects of the K117A and K121A changes were  
320 observed in the context of the E.2 and AE.2 HIV-1<sub>AD8</sub> constructs discussed below (Table  
321 3).

322

323 As Gln 567 is disordered in most Env trimer structures, we used a low-resolution  
324 model of the uncleaved HIV-1<sub>JR-FL</sub> Env (156) to suggest potential interaction partners.  
325 However, alanine substitutions in these potentially interacting HIV-1<sub>AD8</sub> residues (Glu  
326 47, Glu 83, Glu 87, Glu 91, Asp 230, Glu 492 and Glu 560) did not affect the  
327 phenotypes of the Q567K mutant virus (data not shown).

328

### 329 **Q114E and Q567K synergize with other State 1-stabilizing Env changes**

330 Previous studies suggested that changes in His 66, Ala 582 and Leu 587 could enrich  
331 the State-1 HIV-1<sub>YU2</sub> Env conformation through different proposed mechanisms: H66N  
332 destabilizes the CD4-bound conformation, A582T directly stabilizes the pretriggered  
333 conformation and L587A destabilizes the gp41 3-helix bundle (121, 122, 125). We

334 confirmed that individually these changes increased HIV-1<sub>AD8</sub> resistance to cold, sCD4  
335 and BNM-III-170 (Table 2). Of the three changes, only A582T enhanced gp120-trimer  
336 association in cell lysates. Both the H66N and A582T changes synergized with the  
337 Q114E and Q567K changes in producing viral phenotypes associated with State-1  
338 stabilization (Table 2). A combination of three changes in the Q114E/Q567K/A582T  
339 Env resulted in the most robust phenotypes.

340

### 341 **Crosslinkable E.2 and AE.2 Envs with enhanced State-1 stability**

342 To generate HIV-1 Envs enriched in a pretriggered conformation and containing multiple  
343 lysine residues for crosslinking, we added two benign changes (R252K, A667K) and  
344 Q114E to the lysine-rich 2-4 R Env to create the E.2 Env construct (Fig. 1). The AE.2  
345 Env contains, in addition, the A582T change. The A582T change was chosen because  
346 it not only resulted in viral phenotypes additive with those of Q114E and Q567K, but  
347 also increased gp120 association with the detergent-solubilized Env, a property that  
348 K117A, K121A, H66N and L587A lacked (Table 2). Both E.2 and AE.2 Env were  
349 cleaved more efficiently than the wild-type HIV-1<sub>AD8</sub> Env and resisted gp120 dissociation  
350 from the solubilized Env trimer (Fig. 4A). By comparison, the wild-type Env from  
351 another primary strain, HIV-1<sub>JR-FL</sub>, was poorly processed and highly unstable in  
352 detergent.

353

354 To evaluate the functional E.2 and AE.2 Envs in more detail, we tested virus  
355 sensitivity to a panel of broadly and poorly neutralizing antibodies. In addition to the  
356 antibodies used in Figure 2, we included two bNAbs, PGT151 against the gp120-gp41  
357 interface (157) and PGT145 against a quaternary V2 epitope (158), and the poorly

358 neutralizing F240 antibody against gp41 (159). Envs from the Clade B HIV-1<sub>JR-FL</sub> and  
359 Clade A HIV-1<sub>BG505</sub> Tier 2/3 strains were included for comparison. All Env variants  
360 resisted neutralization by poorly neutralizing antibodies, as expected (Fig. 4B).  
361 Compared to the wild-type HIV-1<sub>AD8</sub>, HIV-1<sub>JR-FL</sub> and HIV-1<sub>BG505</sub>, the E.2 and AE.2  
362 viruses were just as sensitive, and even more sensitive in some cases, to neutralization  
363 by broadly neutralizing antibodies.

364

365 The sensitivity of the viruses to cold inactivation, sCD4 and the CD4-mimetic  
366 compound, BNM-III-170, is shown in Fig. 4C. Compared with the wild-type HIV-1<sub>AD8</sub>,  
367 the E.2 virus exhibited increased resistance to cold, sCD4 and BNM-III-170. Alteration  
368 of Glu 114 in the E.2 Env to glutamine largely reverted these phenotypes, suggesting  
369 that the Q114E change is a critical determinant of the stabilized pretriggered  
370 conformation in the E.2 Env (data not shown). The inclusion of the A582T change in  
371 the AE.2 Env further increased cold, sCD4 and BNM-III-170 resistance to the levels of  
372 the Tier 2/3 HIV-1<sub>JR-FL</sub> and HIV-1<sub>BG505</sub> strains. In addition, the E.2 and AE.2 viruses  
373 were more sensitive than the wild-type HIV-1<sub>AD8</sub> to the State 1-preferring entry  
374 inhibitors, BMS-806 and 484 (45, 118); the AE.2 virus was more sensitive to these  
375 small-molecule inhibitors than the E.2 virus (data not shown).

376

377 In an attempt to improve the E.2 and AE.2 Envs further, we added the K59A  
378 and/or V255I changes. Lysine 59 is a highly conserved residue in the gp120 inner  
379 domain, within the disulfide loop (Layer 1) that includes His 66, discussed above.  
380 Valine 255 packs against the critical Trp 112 and Trp 427 residues in the CD4-binding  
381 Phe 43 cavity of gp120 (152); the V255I change was associated with resistance to AAR

382 029b, a cyclic peptide triazole inhibitor of CD4 binding (160). The K59A and V255I  
383 changes alone rendered HIV-1<sub>AD8</sub> more cold-resistant, and the K59A virus was also  
384 relatively resistant to sCD4 and BNM-III-170 (Table 3). However, the K59A and V255I  
385 changes had only modest effects in the E.2 and AE.2 background on State 1-associated  
386 phenotypes, but led to significant reductions in infectivity (Table 3). These observations  
387 hint that further stabilization of State 1-associated phenotypes in the AE.2 context may  
388 be accompanied by decreases in Env function.

389

### 390 **Effects of State 1-destabilizing changes in different Env contexts**

391 In the above studies, the Q114E change could revert the viral phenotypes associated  
392 with State 1 destabilization by the Q203A change but not by changes in the adjacent  
393 Thr 202 residue (Table 2). We evaluated whether an Env with multiple State 1-  
394 stabilizing changes, 2-4 RM6 AE, would better tolerate State 1 destabilization. The 2-4  
395 RM6 AE and AE.2 Envs are identical except for the benign R252K change in the latter  
396 (Fig. 1). The 2-4 RM6 AE virus is resistant to cold, sCD4 and BNM-III-170 and exhibits  
397 a strong gp120-trimer association in detergent (Table 3). We individually introduced the  
398 R542V, I595F and L602H changes into the wild-type HIV-1<sub>AD8</sub> Env or the 2-4 RM6 AE  
399 Env. These gp41 changes rendered HIV-1 more sensitive to the nonpeptidic inhibitory  
400 compound RPR103611, which suggested that they might destabilize the pretriggered  
401 (State-1) Env conformation (161). In agreement with this hypothesis, the R542V and  
402 L602H viruses exhibited increased sensitivity to cold, sCD4 and BNM-III-170 relative to  
403 HIV-1<sub>AD8</sub> (Table 3). The I595F virus was sensitive to sCD4 and BNM-III-170 as well as  
404 to the 19b anti-V3 antibody, but was slightly more resistant to cold inactivation than HIV-  
405 1<sub>AD8</sub>. Interestingly, the increased sensitivity to cold, sCD4, BNM-III-170 and 19b

406 associated with these gp41 changes was not evident in the 2-4 RM6 AE background.  
407 Thus, the State 1- stabilizing changes in 2-4 RM6 AE apparently resist the State 1-  
408 destabilizing effects of the R542V, I595F and L602H changes in the gp41 ectodomain.

409

410 **Correlations among key Env phenotypes**

411 To understand the relationships among key Env phenotypes and to visualize the effects  
412 of specific amino acid changes on the progression of successive generations of Env  
413 mutants, we plotted the relative levels of resistance to cold, BNM-III-170 and gp120-  
414 trimer dissociation for all characterized Env variants (Fig. 5). Virus resistance to cold  
415 inactivation reflects the stability of the functional Env trimer on virions and is  
416 independent of the binding of an Env ligand. Virus resistance to the CD4-mimetic  
417 compound generally correlates with resistance to sCD4 (122,154, 162). Of interest,  
418 there exists a strong correlation between virus resistance to the CD4-mimetic  
419 compound and to cold (Fig. 5). Beginning with the wild-type HIV-1<sub>AD8</sub> Env, Envs  
420 incorporating additive State 1- stabilizing changes displayed upward shifts towards  
421 highly resistant phenotypes, comparable to those of the HIV-1<sub>JR-FL</sub> and HIV-1<sub>BG505</sub> Envs.  
422 Envs with State 1-destabilizing changes grouped together in the lower left quadrant.

423

424 Env variants that exhibited a higher level of gp120-trimer association in  
425 detergent, relative to that of the wild-type HIV-1<sub>AD8</sub> Env, are colored green in Figure 5.  
426 The skewed distribution of these Env variants in the upper right quadrant indicates that  
427 a tighter association of gp120 with the solubilized Env trimer is related to virus  
428 resistance to cold and BNM-III-170, phenotypes associated with State 1 stabilization.  
429 Note that several Env variants, including the natural HIV-1<sub>JR-FL</sub> and HIV-1<sub>BG505</sub> Envs,

430 achieve virus resistance to cold and BNM-III-170 without increasing gp120-trimer  
431 association in detergent-solubilized Envs. Therefore, increasing gp120-trimer  
432 association is not the only means of achieving a more stable pretriggered (State-1) Env  
433 conformation.

434

#### 435 **Crosslinking efficiency of the wild-type AD8, E.2 and AE.2 Envs**

436 The lysine-rich E.2 and AE.2 Envs are expected to crosslink more efficiently than the  
437 wild-type HIV-1<sub>AD8</sub> Env with lysine-reactive crosslinkers like DTSSP and glutaraldehyde.  
438 DTSSP has a spacer arm of 12 Å, whereas, because of its tendency to polymerize,  
439 glutaraldehyde forms crosslinks of more variable lengths (163). Both DTSSP and  
440 glutaraldehyde crosslinked the E.2 and AE.2 Envs more efficiently than the wild-type  
441 AD8 Env (Fig. 6A). For example, after treatment with 5 mM glutaraldehyde, the E.2 and  
442 AE.2 Envs crosslinked into gel-stable trimers, whereas the wild-type HIV-1<sub>AD8</sub> Env  
443 mostly formed monomers and dimers. Apparently, a greater number of lysine residues  
444 accessible to the crosslinkers exist on the surface of the E.2 and AE.2 Env trimers  
445 compared with the wild-type HIV-1<sub>AD8</sub> Env.

446

447 We also examined the relative sensitivity of the functional wild-type HIV-1<sub>AD8</sub>, E.2  
448 and AE.2 Envs to BS3, another lysine-specific crosslinker with spacer arms of 12 Å.  
449 The infectivity of viruses pseudotyped with the E.2 and AE.2 Envs was inhibited by BS3  
450 at three- to four-fold lower concentrations than those required for inhibition of viruses  
451 with the wild-type HIV-1<sub>AD8</sub> Env (Fig. 6B). These results suggest that BS3 crosslinks  
452 occur more efficiently on the E.2 and AE.2 Envs than on the wild-type HIV-1<sub>AD8</sub> Env,  
453 leading to a loss of infectivity at lower BS3 concentrations.

454 **DISCUSSION**

455 Despite more than three decades of intense research, an effective HIV-1 vaccine  
456 remains elusive. The metastability and multiple conformational states of the HIV-1 Env  
457 create challenges for the generation of broadly neutralizing antibodies, either following  
458 vaccination or during natural HIV-1 infection. In Env-expressing cells, both uncleaved  
459 and cleaved (mature) Envs are present on the cell surface. A significant fraction of the  
460 uncleaved Env bypasses the conventional Golgi secretory pathway to traffic to the cell  
461 surface; these Envs differ from mature Envs in glycan processing, conformation and  
462 recognition by antibodies (7). Uncleaved Envs may function as a decoy to the host  
463 immune system and divert antibody responses away from the mature Envs. The  
464 pretriggered (State-1) conformation of the mature virion Env of primary HIV-1 strains is  
465 the target for most broadly neutralizing antibodies (12, 37, 38, 45). This native  
466 conformation, however, is unstable and can transition into more open State 2/3  
467 conformations that are able to be recognized by poorly neutralizing antibodies.  
468 Therefore, it is of significant interest to devise methods to lock Env in its native State-1  
469 conformation by means that resist perturbation during Env purification, characterization  
470 and immunization.

471

472 Here, we tackled the challenges posed by HIV-1 Env conformational flexibility in  
473 two ways. First, we used polymorphisms in naturally occurring HIV-1 strains to guide  
474 the introduction of extra lysine and acidic amino acid residues in the HIV-1<sub>AD8</sub> Env.  
475 Chemical crosslinkers that couple lysine or acidic residues on proteins under  
476 physiological conditions are available (132-135). During the iterative process employed  
477 to identify HIV-1<sub>AD8</sub> Envs that are potentially more susceptible to crosslinking, we

478 required that the Env variants exhibit efficient processing, subunit association, and the  
479 ability to support virus entry. Some of the functional HIV-1<sub>AD8</sub> Env variants developed  
480 by this approach contain up to 11 extra lysine residues (33 per Env trimer) and up to 7  
481 extra acidic residues (21 per Env trimer). Using DTSSP or glutaraldehyde as  
482 crosslinking agents, two Env variants, E.2 and AE.2, were shown to form interprotomer  
483 crosslinks more efficiently than the wild-type HIV-1<sub>AD8</sub> Env. The infectivity of viruses  
484 with these Envs was inactivated more efficiently than that of viruses with the wild-type  
485 HIV-1<sub>AD8</sub> Env by another lysine-specific crosslinker, BS3. These assays document the  
486 accessibility of some of the additional lysine residues introduced into the E.2 and AE.2  
487 Envs. Chemical crosslinking can enrich the representation of labile native  
488 conformations in Env preparations for structural analysis or immunogenicity studies.  
489 Crosslinking/mass spectrometry can provide distance constraints between Env residues  
490 that can be used to validate available structural models or to derive new models (132-  
491 135). A previous study utilized crosslinking/mass spectrometry to detect differences  
492 between soluble and membrane-bound Envs (73). The inclusion of the 2-4 RED2, E.2  
493 and AE.2 Envs in future crosslinking/mass spectrometry studies should increase the  
494 number of distance constraints and thereby improve our ability to discriminate among  
495 alternative structural models.

496

497 The second strategy employed in our approach was to screen the Env variants  
498 for function and viral phenotypes associated with stabilization of a State-1 Env  
499 conformation. For this purpose, we evaluated viral resistance to cold, sCD4 and the  
500 CD4-mimetic compound BNM-III-170. Cold inactivation reflects the resistance of the  
501 functional HIV-1 Env trimer to the detrimental effects of ice formation at near-freezing

502 temperatures (164-166). The sensitivity of HIV-1 variants to cold inactivation is related  
503 to the intrinsic reactivity or triggerability of Env; Envs that more readily make the  
504 transition from State 1 to downstream conformations are invariably cold-sensitive (23,  
505 121, 122). HIV-1 sensitivity to sCD4 and BNM-III-170 inhibition is a function of Env  
506 triggerability (23, 45, 118, 119, 125); because we generally avoided changes to the  
507 highly conserved and well-defined BNM-III-170 binding site on gp120 (151, 162), most  
508 of the observed differences in virus sensitivity to this CD4-mimetic compound reflect  
509 changes in the ability of Env to negotiate transitions from a State-1 conformation. Our  
510 study documents the strong correlation between HIV-1 resistance to cold and resistance  
511 to BNM-III-170. This screening strategy identified two changes, Q114E in gp120 and  
512 Q567K in gp41, that individually increased the resistance of the HIV-1<sub>AD8</sub> Env to  
513 inactivation by cold, sCD4 and BNM-III-170. These viral phenotypes were additively  
514 enhanced by combining the Q114E and Q567K changes in Env variants, such as the  
515 lysine-rich E.2 and AE.2 Envs. Cold, sCD4 and BNM-III-170 resistance were further  
516 increased by the inclusion in the AE.2 Env of the A582T gp41 change, which previously  
517 was shown to stabilize a pretriggered Env conformation (123, 125). The functional E.2  
518 and AE.2 Envs exhibit an antigenic profile consistent with a State-1 conformation,  
519 conferring virus sensitivity to broadly neutralizing antibodies that target quaternary  
520 epitopes (PG16, PGT145, PGT151, 35O22) and resistance to poorly neutralizing  
521 antibodies (17b, 19b, 902090, F105, F240). Viruses with the E.2 and AE.2 Envs were  
522 inhibited efficiently by BMS-806, a small molecule that exhibits some preference for a  
523 State-1 Env conformation (12, 78, 138-140). Two unanticipated beneficial phenotypes  
524 associated with the E.2 and AE.2 Envs are more efficient Env processing and greater  
525 stability of solubilized Env trimers. HIV-1 Env cleavage has been suggested to

526 contribute to the stability of the State-1 conformation (138, 139, 167-173). As  
527 uncleaved HIV-1 Envs sample multiple conformations, including those reactive with  
528 poorly neutralizing antibodies, achieving a high level of gp120-gp41 processing may be  
529 important for an effective vaccine immunogen. The E.2 and AE.2 Envs achieve levels  
530 of State 1- associated phenotypes comparable to those of the Tier 2/3 HIV-1<sub>JR-FL</sub> and  
531 HIV-1<sub>BG505</sub>, but notably, are processed much more efficiently. In addition, relative to  
532 these Envs and the wild-type HIV-1<sub>AD8</sub> Env, the E.2 and AE.2 Envs solubilized in  
533 detergent exhibit much greater gp120 association with the Env trimer. The Q114E,  
534 Q567K and A582T changes individually strengthen the non-covalent association of  
535 gp120 with the solubilized Env trimers, a property that will assist purification and  
536 characterization. Of interest, the Q567K change was included in a combination of Env  
537 changes that were reported to stabilize HIV-1 Env trimers in different contexts (174-  
538 176). In our panel of HIV-1 Env variants, enhancement of Env trimer stability in  
539 detergent was strongly correlated with virus resistance to cold and BNM-III-170, State 1-  
540 associated phenotypes. We note that the binding of the State 1-preferring compound,  
541 BMS-806, also stabilizes gp120-trimer association (138). In future studies, the ability of  
542 Q114E, Q567K and A582T changes to enhance Env cleavage efficiency, gp120-trimer  
543 association and State-1 stabilization in other HIV-1 strains will be explored.

544

545 We identified other changes (K59A, K117A, K121A) that individually yielded Env  
546 phenotypes consistent with State-1 stabilization. These and previously identified State  
547 1-stabilizing changes (H66N, L587A) (121, 122, 125) were tested in combination with  
548 the Q114E and/or Q567K changes in various Env backgrounds. In no case did we  
549 observe an additive improvement in viral phenotypes associated with State 1

550 stabilization, and several of these combinations resulted in attenuated virus replication  
551 or gp120-trimer dissociation in detergent. It is not surprising that, as State 1 stability is  
552 increased, virus replication diminishes as the activation barriers governing State 1-to-  
553 State 2 transitions increase. However, the validation of State 1 stabilization would be  
554 less straightforward for replication-incompetent Envs, given current uncertainties about  
555 a State-1 Env structure. Therefore, we deferred investigation of these potentially State-  
556 1-stabilizing changes until better assays to characterize the conformations of  
557 nonfunctional Envs are established.

558

559 Changes in gp41 (I559P, L555P) that are intended to prevent the formation of the  
560 HR1 coiled coil have been used to stabilize soluble gp140 trimers (70, 88, 177).  
561 However, introduction of these changes in combination with the major State 1-  
562 stabilizing changes (Q114E/I559P, Q114E/Q567K/I559P and Q114E/Q567K/L555P)  
563 resulted in Envs that were not processed (data not shown).

564

565 We also considered another gp41 change, Q658E, that has been shown to  
566 stabilize sgp140 SOSIP.664 trimers (178). Introduction of the Q658E change into the  
567 wild-type HIV-1<sub>AD8</sub> Env resulted in increased virus sensitivity to cold, sCD4, BNM-III-170  
568 and the 19b antibody (data not shown). These phenotypes are consistent with those  
569 reported in other HIV-1 strains (178) and, as they suggest a lower occupancy of State 1,  
570 we did not evaluate the Q658E change in combination with the Q114E and Q567K  
571 changes.

572

573            Although a State-1 Env structure is currently unknown, mapping the Env residues  
574    identified in this study on available Env trimer models can provide some insights.  
575    Figure 7 shows the locations of Env residues in which changes resulted in increases or  
576    decreases in State 1-associated phenotypes on a PGT151-bound HIV-1<sub>JR-FL</sub> EnvΔCT  
577    trimer (PDB: 5FUU) (82). The binding of the PGT151 antibody induces a State-2  
578    conformation that is asymmetric, with two antibody Fabs bound to the Env trimer (78,  
579    82). We chose this structure because, unlike most HIV-1 trimer structures, the HR1<sub>N</sub>  
580    region containing Gln 567 is resolved; however, in keeping with the asymmetry of the  
581    PGT151-bound Env trimer, the positions of the Gln 567 residues differ among the three  
582    Env protomers. Gln 567, Gln 114, and Ala 582 are close to the trimer axis in the  
583    EnvΔCT structure (Fig. 7A). The C<sub>α</sub>-C<sub>α</sub> distances between Gln 114 and Gln 567  
584    residues vary from 11.6 to 15.2 Å and the side chains of these residues do not  
585    apparently interact in this Env conformation. Gln 114 is stacked above Lys 117 and Lys  
586    121, the side chains of which project towards the Env trimer axis (Fig. 7B, right panel).  
587    Although a precise structural explanation for the observed State 1-stabilizing  
588    phenotypes will require more data, the implicated residues are positioned near  
589    intersubunit or interprotomer junctions and therefore could potentially modulate trimer  
590    opening. For example, electrostatic repulsion among Lys 117 residues that destabilizes  
591    the Env trimer could be mitigated by their conversion to alanine residues or by replacing  
592    Gln114 with acidic residues.

593

594            The State 1-destabilizing changes identified in this study (red residues in Fig. 7B,  
595    left panel) are less localized than the State 1-stabilizing changes (green and yellow  
596    residues in Fig. 7B, left panel). This is consistent with the expectation that a metastable

597 structure can be disrupted by a diverse set of changes, whereas a more limited and  
598 strategically placed set of changes is required to strengthen the structure. In this study,  
599 we provide an example of how State 1-stabilizing changes in Env can counter the  
600 phenotypic effects of State 1-destabilizing alterations, even when these changes involve  
601 amino acid residues very distant on current Env trimer structures.

602

603 In a related paper, we report the ability of the State 1-stabilizing changes  
604 identified herein to counter the phenotypic consequences of disruption of the gp41  
605 MPER. Although further work will be required to understand fully the mechanisms  
606 underlying these observations, the ability of the Q114E, Q567K and A582T changes to  
607 counteract the disruptive effects of distant changes suggests that they may have  
608 significant utility in preserving pretriggered Env conformations in multiple circumstances.

609

## 610 MATERIALS AND METHODS

611 Env glycoprotein constructs. The HIV-1<sub>AD8</sub> and HIV-1<sub>JR-FL</sub> Envs were coexpressed with  
612 the Rev protein in the pSVIIIenv expression vector, using the natural HIV-1 *env* and *rev*  
613 sequences (23). The Asp 718 (Kpn I)-BamHI fragment of HIV-1<sub>AD8</sub> *env* was cloned into  
614 the corresponding sites of the pSVIIIenv plasmid expressing the HIV-1<sub>HxBc2</sub> Env and  
615 Rev. The initial single, double and triple sets of lysine substitutions shown in Fig. 1A  
616 were introduced into the HIV-1<sub>AD8</sub> Env lacking an epitope tag. A carboxy-terminal  
617 GGHHHHHH (His<sub>6</sub>) epitope tag was added to the Env variants shown in Fig. 1B and  
618 derivatives thereof. The mutations were introduced by site-directed PCR mutagenesis  
619 using Pfu Ultra II polymerase (Agilent Technologies), according to the manufacturer's  
620 protocol. The plasmid expressing the HIV-1<sub>BG505</sub> Env (BG505.W6M.ENV.C2) was

621 obtained through the NIH HIV Reagent Program and was contributed by Dr. Julie  
622 Overbaugh.

623

624 Cell lines. 293T cells (ATCC) and HOS cells (ATCC) were grown in Dulbecco's  
625 Modified Eagle's Medium/Nutrient Mixture F12 (DMEM-F12) supplemented with 10%  
626 fetal bovine serum (FBS) and 100 µg/ml of penicillin-streptomycin. A549 cells  
627 expressing HIV-1 Envs with Gag-mCherry fusion proteins were grown in DMEM-F12  
628 medium supplemented with 10% FBS, 1X Pen-Strep, 1X L-glutamine and 0.2%  
629 Amphotericin B. Cf2Th cells stably expressing the human CD4 and CCR5 coreceptors  
630 for HIV-1 were grown in the same medium supplemented with 0.4 mg/ml of G418 and  
631 0.2 mg/ml of hygromycin. All cell culture reagents are from Life Technologies.

632

633 Env processing and gp120-trimer association in Ni-NTA precipitation assay. HOS cells  
634 were cotransfected with a Rev/Env-encoding pSVIIIenv plasmid and a Tat-encoding  
635 plasmid at a 1:0.125 ratio using the Effectene transfection reagent (Qiagen). At 48 h  
636 after transfection, HOS cells were washed with 1X PBS and lysed in 100 mM  
637 (NH<sub>4</sub>)<sub>2</sub>SO<sub>4</sub>, 20 mM Tris-HCl, pH 8, 300 mM NaCl and 1.5% Cymal-5 (Anatrace)  
638 containing DMSO, 10 µM BMS-806 or 10 µg/mL soluble CD4-Ig. Lysates were clarified  
639 and aliquots were saved as the input samples. The remaining lysates were incubated  
640 with nickel-nitriloacetic acid (Ni-NTA) beads (Qiagen) for 1.5 h at 4°C. The beads were  
641 gently pelleted and washed 3 times with room temperature washing buffer (100 mM  
642 (NH<sub>4</sub>)<sub>2</sub>SO<sub>4</sub>, 20 mM Tris-HCl, pH 8, 1 M NaCl and 0.5% Cymal-5). The beads were then  
643 boiled in LDS sample buffer, and the proteins analyzed by Western blotting using  
644 1:2,000 goat anti-gp120 polyclonal antibody (Thermo Fisher Scientific) and 1:2,000

645 HRP-conjugated rabbit anti-goat IgG (Thermo Fisher Scientific) or 4E10 anti-gp41  
646 antibody (Polymun) and 1:2,000 HRP-conjugated goat anti-human IgG (Santa Cruz).

647

648 Virus infectivity, neutralization and cold sensitivity. Single-round virus infection assays  
649 were used to measure the ability of the Env variants to support virus entry, as described  
650 previously (23). Briefly, 293T cells were cotransfected with the Rev/Env-encoding  
651 pSVIIIenv plasmid; a Tat-encoding plasmid; the pCMV HIV-1 Gag-Pol packaging  
652 construct; and a plasmid containing the luciferase-expressing HIV-1 vector at a weight  
653 ratio of 1:0.125:1:3 using a standard calcium phosphate transfection protocol. At 48 h  
654 after transfection, virus-containing supernatants were collected, filtered through a 0.45-  
655 µm membrane, and incubated with soluble CD4, BNM-III-170 or antibody for 1 h at  
656 37°C. The mixture was then added to Cf2Th-CD4/CCR5 cells, which were cultured at  
657 37°C/5% CO<sub>2</sub>. To enhance infection by recombinant viruses with the HIV-1<sub>BG505</sub> Env,  
658 virus-antibody mixtures were spinoculated with target cells at 1800 rpm for one hour at  
659 room temperature and then incubated for one more hour before additional medium was  
660 added. Luciferase activity in the Cf2Th-CD4/CCR5 target cells was measured 48 h later.  
661 To measure cold sensitivity, the viruses were incubated on ice for various lengths of  
662 time prior to measuring their infectivity. To measure the sensitivity of virus infectivity to  
663 crosslinking, the viruses were incubated with BS3 (Thermo Fisher Scientific) for 15  
664 minutes at room temperature; the reaction was quenched with 15 mM Tris-HCl, pH 8.0  
665 for 10 minutes, and the mixture was then added to the target cells.

666

667 Crosslinking of Envs on virus-like particles (VLPs). A549 cells inducibly expressing  
668 virus-like particles (VLPs) consisting of the HIV-1 Gag-mCherry fusion protein and the

669 wild-type HIV-1<sub>AD8</sub> Env have been previously described (7, 138). The D1253 A549-  
670 Gag/Env cell line expressing VLPs with wild-type HIV-1<sub>AD8</sub> Env was selected by FACS  
671 sorting for Gag-positive and PGT145-positive cells. The D1555.042321.sort A549-  
672 Gag/E.2 Env cells and the D1553.042321.sort A549-Gag/AE.2 Env cells inducibly  
673 expressing VLPs with the E.2 and AE.2 Envs, respectively, were established similarly.  
674 After FACS sorting, these cells were >90% dual-positive for Gag expression (KC567  
675 antibody-positive) and Env expression (PGT145 antibody-positive).

676

677 An equivalent number of cells from the three cell lines described above were  
678 seeded and the expression of Gag-mCherry/Env VLPs was induced with 2 µg/ml  
679 doxycycline. Forty-eight to seventy-two hours later, supernatants containing VLPs were  
680 centrifuged at low speed to remove cell debris and then filtered (0.45 µm). Clarified  
681 supernatants were centrifuged at 100,000 x g for one hour at 4°C. VLP pellets were  
682 resuspended in 1X PBS, aliquoted and incubated with different concentrations of either  
683 DTSSP (Thermo Fisher Scientific) or glutaraldehyde crosslinkers. The crosslinking  
684 reaction with DTSSP was carried out for 30 minutes at room temperature, after which  
685 the reaction was quenched with 100 mM Tris-HCl, pH 8.0 for 10 minutes at room  
686 temperature. Glutaraldehyde crosslinking was carried out for 5 minutes at room  
687 temperature, after which the reaction was quenched with 50 mM glycine for 10 minutes  
688 at room temperature. VLPs were then pelleted at 20,000 x g for 30 minutes at 4°C.  
689 VLP pellets were resuspended in 1X PBS/LDS, boiled and Western blotted with a goat  
690 anti-gp120 antibody, as described above. The intensity of the gp120, gp160, dimer and  
691 trimer bands was quantified using the BioRad Image Lab program.

692

693

694 **ACKNOWLEDGMENTS**

695 We thank Ms. Elizabeth Carpelan for manuscript preparation. Antibodies against HIV-1  
696 were kindly supplied by Dennis Burton (Scripps), Peter Kwong and John Mascola  
697 (Vaccine Research Center NIH), Barton Haynes (Duke University), Hermann Katinger  
698 (Polymun), James Robinson (Tulane University), and Marshall Posner (Mount Sinai  
699 Medical Center). We thank the NIH HIV Reagent Program for providing additional  
700 reagents.

701

702 This work was supported by grants from the National Institutes of Health (grants  
703 AI145547, AI124982 and AI150471, including the Basic Science Core of the University  
704 of Alabama Center for AIDS Research (AI27767)) and by a gift from the late William F.  
705 McCarty-Cooper.

706

707

708 **CONFLICT OF INTEREST**

709 The authors declare no conflicts of interest.

710

711 **REFERENCES**

- 713 1. Allan JS, Coligan JE, Barin F, McLane MF, Sodroski JG, Rosen CA, Haseltine  
714 WA, Lee TH, Essex M. 1985. Major glycoprotein antigens that induce antibodies  
715 in AIDS patients are encoded by HTLV-III. *Science* 228:1091-4.
- 716 2. Wyatt R, Sodroski J. 1998. The HIV-1 envelope glycoproteins: fusogens,  
717 antigens, and immunogens. *Science* 280:1884-8.
- 718 3. Fennie C, Lasky LA. 1989. Model for intracellular folding of the human  
719 immunodeficiency virus type 1 gp120. *J Virol* 63:639-46.
- 720 4. Li Y, Luo L, Thomas DY, Kang CY. 2000. The HIV-1 Env protein signal sequence  
721 retards its cleavage and down-regulates the glycoprotein folding. *Virology*  
722 272:417-28.
- 723 5. Willey RL, Bonifacino JS, Potts BJ, Martin MA, Klausner RD. 1988. Biosynthesis,  
724 cleavage, and degradation of the human immunodeficiency virus 1 envelope  
725 glycoprotein gp160. *Proc Natl Acad Sci U S A* 85:9580-4.
- 726 6. Earl PL, Moss B, Doms RW. 1991. Folding, interaction with GRP78-BiP,  
727 assembly, and transport of the human immunodeficiency virus type 1 envelope  
728 protein. *J Virol* 65:2047-55.
- 729 7. Zhang S, Nguyen HT, Ding H, Wang J, Zou S, Liu L, Guha D, Gabuzda D, Ho  
730 DD, Kappes JC, Sodroski J. 2021. Dual pathways of human immunodeficiency  
731 virus type 1 envelope glycoprotein trafficking modulate the selective exclusion of  
732 uncleaved oligomers from virions. *J Virol* 95:e01369-20.
- 733 8. Doores KJ, Bonomelli C, Harvey DJ, Vasiljevic S, Dwek RA, Burton DR, Crispin  
734 M, Scanlan CN. 2010. Envelope glycans of immunodeficiency virions are almost  
735 entirely oligomannose antigens. *Proc Natl Acad Sci U S A* 107:13800-5.
- 736 9. Go EP, Herschhorn A, Gu C, Castillo-Menendez L, Zhang S, Mao Y, Chen H,  
737 Ding H, Wakefield JK, Hua D, Liao HX, Kappes JC, Sodroski J, Desaire H. 2015.  
738 Comparative analysis of the glycosylation profiles of membrane-anchored HIV-1  
739 envelope glycoprotein trimers and soluble gp140. *J Virol* 89:8245-57.
- 740 10. Merkle RK, Helland DE, Welles JL, Shilatifard A, Haseltine WA, Cummings RD.  
741 1991. gp160 of HIV-1 synthesized by persistently infected Molt-3 cells is  
742 terminally glycosylated: evidence that cleavage of gp160 occurs subsequent to  
743 oligosaccharide processing. *Arch Biochem Biophys* 290:248-57.
- 744 11. Brakch N, Dettin M, Scarinci C, Seidah NG, Di Bello C. 1995. Structural  
745 investigation and kinetic characterization of potential cleavage sites of HIV  
746 GP160 by human furin and PC1. *Biochem Biophys Res Commun* 213:356-61.

758 12. Munro JB, Gorman J, Ma X, Zhou Z, Arthos J, Burton DR, Koff WC, Courter JR,  
759 Smith AB III, Kwong PD, Blanchard SC, Mothes W. 2014. Conformational  
760 dynamics of single HIV-1 envelope trimers on the surface of native virions.  
761 Science 346:759-63.

762

763 13. Dalglish AG, Beverley PC, Clapham PR, Crawford DH, Greaves MF, Weiss RA.  
764 1984. The CD4 (T4) antigen is an essential component of the receptor for the  
765 AIDS retrovirus. Nature 312:763-7.

766

767 14. Cocchi F, DeVico AL, Garzino-Demo A, Arya SK, Gallo RC, Lusso P. 1995.  
768 Identification of RANTES, MIP-1 alpha, and MIP-1 beta as the major HIV-  
769 suppressive factors produced by CD8+ T cells. Science 270:1811-5.

770

771 15. Deng H, Liu R, Ellmeier W, Choe S, Unutmaz D, Burkhardt M, Di Marzio P,  
772 Marmon S, Sutton RE, Hill CM, Davis CB, Peiper SC, Schall TJ, Littman DR,  
773 Landau NR. 1996. Identification of a major co-receptor for primary isolates of  
774 HIV-1. Nature 381:661-6.

775

776 16. Feng Y, Broder CC, Kennedy PE, Berger EA. 1996. HIV-1 entry cofactor:  
777 functional cDNA cloning of a seven-transmembrane, G protein-coupled receptor.  
778 Science 272:872-7.

779

780 17. Alkhatib G, Combadiere C, Broder CC, Feng Y, Kennedy PE, Murphy PM,  
781 Berger EA. 1996. CC CKR5: a RANTES, MIP-1alpha, MIP-1beta receptor as a  
782 fusion cofactor for macrophage-tropic HIV-1. Science 272:1955-8.

783

784 18. Choe H, Farzan M, Sun Y, Sullivan N, Rollins B, Ponath PD, Wu L, Mackay CR,  
785 LaRosa G, Newman W, Gerard N, Gerard C, Sodroski J. 1996. The beta-  
786 chemokine receptors CCR3 and CCR5 facilitate infection by primary HIV-1  
787 isolates. Cell 85:1135-48.

788

789 19. Doranz BJ, Rucker J, Yi Y, Smyth RJ, Samson M, Peiper SC, Parmentier M,  
790 Collman RG, Doms RW. 1996. A dual-tropic primary HIV-1 isolate that uses fusin  
791 and the beta-chemokine receptors CKR-5, CKR-3, and CKR-2b as fusion  
792 cofactors. Cell 85:1149-58.

793

794 20. Dragic T, Litwin V, Allaway GP, Martin SR, Huang Y, Nagashima KA, Cayanan  
795 C, Madden PJ, Koup RA, Moore JP, Paxton WA. 1996. HIV-1 entry into CD4+  
796 cells is mediated by the chemokine receptor CC-CKR-5. Nature 381:667-73.

797

798 21. Wu L, Gerard NP, Wyatt R, Choe H, Parolin C, Ruffing N, Borsetti A, Cardoso  
799 AA, Desjardin E, Newman W, Gerard C, Sodroski J. 1996. CD4-induced  
800 interaction of primary HIV-1 gp120 glycoproteins with the chemokine receptor  
801 CCR-5. Nature 384:179-83.

802

803 22. Trkola A, Dragic T, Arthos J, Binley JM, Olson WC, Allaway GP, Cheng-Mayer C,  
804 Robinson J, Madden PJ, Moore JP. 1996. CD4-dependent, antibody-sensitive

805 interactions between HIV-1 and its co-receptor CCR-5. *Nature* 384:184-7.

806

807 23. Haim H, Strack B, Kassa A, Madani N, Wang L, Courter JR, Princiotto A, McGee  
808 K, Pacheco B, Seaman MS, Smith AB III, Sodroski J. 2011. Contribution of  
809 intrinsic reactivity of the HIV-1 envelope glycoproteins to CD4-independent  
810 infection and global inhibitor sensitivity. *PLoS Pathog* 7:e1002101.

811

812 24. Ma X, Lu M, Gorman J, Terry DS, Hong X, Zhou Z, Zhao H, Altman RB, Arthos J,  
813 Blanchard SC, Kwong PD, Munro JB, Mothes W. 2018. HIV-1 Env trimer opens  
814 through an asymmetric intermediate in which individual protomers adopt distinct  
815 conformations. *Elife* 7:e34271.

816

817 25. Khasnis MD, Halkidis K, Bhardwaj A, Root MJ. 2016. Receptor activation of HIV-  
818 1 Env leads to asymmetric exposure of the gp41 trimer. *PLoS Pathog*  
819 12:e1006098.

820

821 26. Liu J, Bartesaghi A, Borgnia MJ, Sapiro G, Subramaniam S. 2008. Molecular  
822 architecture of native HIV-1 gp120 trimers. *Nature* 455:109-13.

823

824 27. Wang H, Cohen AA, Galimidi RP, Gristick HB, Jensen GJ, Bjorkman PJ. 2016.  
825 Cryo-EM structure of a CD4-bound open HIV-1 envelope trimer reveals structural  
826 rearrangements of the gp120 V1V2 loop. *Proc Natl Acad Sci U S A* 113:E7151-  
827 E7158.

828

829 28. Ozorowski G, Pallesen J, de Val N, Lyumkis D, Cottrell CA, Torres JL, Copps J,  
830 Stanfield RL, Cupo A, Pugach P, Moore JP, Wilson IA, Ward AB. 2017. Open  
831 and closed structures reveal allostery and pliability in the HIV-1 envelope spike.  
832 *Nature* 547:360-63.

833

834 29. Furuta RA, Wild CT, Weng Y, Weiss CD. 1998. Capture of an early fusion-active  
835 conformation of HIV-1 gp41. *Nat Struct Biol* 5:276-9.

836

837 30. Koshiba T, Chan DC. 2003. The prefusogenic intermediate of HIV-1 gp41  
838 contains exposed C-peptide regions. *J Biol Chem* 278:7573-9.

839

840 31. He Y, Vassell R, Zaitseva M, Nguyen N, Yang Z, Weng Y, Weiss CD. 2003.  
841 Peptides trap the human immunodeficiency virus type 1 envelope glycoprotein  
842 fusion intermediate at two sites. *J Virol* 77:1666-71.

843

844 32. Chan DC, Fass D, Berger JM, Kim PS. 1997. Core structure of gp41 from the  
845 HIV envelope glycoprotein. *Cell* 89:263-73.

846

847 33. Weissenhorn W, Dessen A, Harrison SC, Skehel JJ, Wiley DC. 1997. Atomic  
848 structure of the ectodomain from HIV-1 gp41. *Nature* 387:426-30.

849

850 34. Lu M, Blacklow SC, Kim PS. 1995. A trimeric structural domain of the HIV-1  
851 transmembrane glycoprotein. *Nat Struct Biol* 2:1075-82.

852  
853 35. Melikyan GB, Markosyan RM, Hemmati H, Delmedico MK, Lambert DM, Cohen  
854 FS. 2000. Evidence that the transition of HIV-1 gp41 into a six-helix bundle, not  
855 the bundle configuration, induces membrane fusion. *J Cell Biol* 151:413-23.  
856  
857 36. Wilen CB, Tilton JC, Doms RW. 2012. Molecular mechanisms of HIV entry. *Adv  
858 Exp Med Biol* 726:223-42.  
859  
860 37. Haim H, Salas I, McGee K, Eichelberger N, Winter E, Pacheco B, Sodroski J.  
861 2013. Modeling virus- and antibody-specific factors to predict human  
862 immunodeficiency virus neutralization efficiency. *Cell Host Microbe* 14:547-58.  
863  
864 38. Guttman M, Cupo A, Julien JP, Sanders RW, Wilson IA, Moore JP, Lee KK.  
865 2015. Antibody potency relates to the ability to recognize the closed, pre-fusion  
866 form of HIV Env. *Nat Commun* 6:6144.  
867  
868 39. Kwong PD, Doyle ML, Casper DJ, Cicala C, Leavitt SA, Majeed S, Steenbeke  
869 TD, Venturi M, Chaiken I, Fung M, Katinger H, Parren PW, Robinson J, Van Ryk  
870 D, Wang L, Burton DR, Freire E, Wyatt R, Sodroski J, Hendrickson WA, Arthos J.  
871 2002. HIV-1 evades antibody-mediated neutralization through conformational  
872 masking of receptor-binding sites. *Nature* 420:678-82.  
873  
874 40. Wei X, Decker JM, Wang S, Hui H, Kappes JC, Wu X, Salazar-Gonzalez JF,  
875 Salazar MG, Kilby JM, Saag MS, Komarova NL, Nowak MA, Hahn BH, Kwong  
876 PD, Shaw GM. 2003. Antibody neutralization and escape by HIV-1. *Nature*  
877 422:307-12.  
878  
879 41. Decker JM, Bibollet-Ruche F, Wei X, Wang S, Levy DN, Wang W, Delaporte E,  
880 Peeters M, Derdeyn CA, Allen S, Hunter E, Saag MS, Hoxie JA, Hahn BH,  
881 Kwong PD, Robinson JE, Shaw GM. 2005. Antigenic conservation and  
882 immunogenicity of the HIV coreceptor binding site. *J Exp Med* 201:1407-19.  
883  
884 42. Alsahafi N, Bakouche N, Kazemi M, Richard J, Ding S, Bhattacharyya S, Das D,  
885 Anand SP, Prevost J, Tolbert WD, Lu H, Medjahed H, Gendron-Lepage G,  
886 Ortega Delgado GG, Kirk S, Melillo B, Mothes W, Sodroski J, Smith AB III,  
887 Kaufmann DE, Wu X, Pazgier M, Rouiller I, Finzi A, Munro JB. 2019. An  
888 asymmetric opening of HIV-1 envelope mediates antibody-dependent cellular  
889 cytotoxicity. *Cell Host Microbe* 25:578-87 e5.  
890  
891 43. Labrijn AF, Poignard P, Raja A, Zwick MB, Delgado K, Franti M, Binley J, Vivona  
892 V, Grundner C, Huang CC, Venturi M, Petropoulos CJ, Wrin T, Dimitrov DS,  
893 Robinson J, Kwong PD, Wyatt RT, Sodroski J, Burton DR. 2003. Access of  
894 antibody molecules to the conserved coreceptor binding site on glycoprotein  
895 gp120 is sterically restricted on primary human immunodeficiency virus type 1. *J  
896 Virol* 77:10557-65.  
897  
898 44. Moore PL, Ranchobe N, Lambson BE, Gray ES, Cave E, Abrahams MR,

899 Bandawe G, Mlisana K, Abdoool Karim SS, Williamson C, Morris L, Study C,  
900 Immunology NCfHAV. 2009. Limited neutralizing antibody specificities drive  
901 neutralization escape in early HIV-1 subtype C infection. PLoS Pathog  
902 5:e1000598.

903

904 45. Herschhorn A, Ma X, Gu C, Ventura JD, Castillo-Menendez L, Melillo B, Terry  
905 DS, Smith AB III, Blanchard SC, Munro JB, Mothes W, Finzi A, Sodroski J. 2016.  
906 Release of gp120 Restraints Leads to an Entry-Competent Intermediate State of  
907 the HIV-1 Envelope Glycoproteins. mBio 7:e01598-16.

908

909 46. Wibmer CK, Bhiman JN, Gray ES, Tumba N, Abdoool Karim SS, Williamson C,  
910 Morris L, Moore PL. 2013. Viral escape from HIV-1 neutralizing antibodies drives  
911 increased plasma neutralization breadth through sequential recognition of  
912 multiple epitopes and immunotypes. PLoS Pathog 9:e1003738.

913

914 47. Gray ES, Taylor N, Wycuff D, Moore PL, Tomaras GD, Wibmer CK, Puren A,  
915 DeCamp A, Gilbert PB, Wood B, Montefiori DC, Binley JM, Shaw GM, Haynes  
916 BF, Mascola JR, Morris L. 2009. Antibody specificities associated with  
917 neutralization breadth in plasma from human immunodeficiency virus type 1  
918 subtype C-infected blood donors. J Virol 83:8925-37.

919

920 48. Sather DN, Armann J, Ching LK, Mavrantoni A, Sellhorn G, Caldwell Z, Yu X,  
921 Wood B, Self S, Kalams S, Stamatatos L. 2009. Factors associated with the  
922 development of cross-reactive neutralizing antibodies during human  
923 immunodeficiency virus type 1 infection. J Virol 83:757-69.

924

925 49. Klein F, Diskin R, Scheid JF, Gaebler C, Mouquet H, Georgiev IS, Pancera M,  
926 Zhou T, Incesu RB, Fu BZ, Gnanapragasam PN, Oliveira TY, Seaman MS,  
927 Kwong PD, Bjorkman PJ, Nussenzweig MC. 2013. Somatic mutations of the  
928 immunoglobulin framework are generally required for broad and potent HIV-1  
929 neutralization. Cell 153:126-38.

930

931 50. Walker LM, Simek MD, Priddy F, Gach JS, Wagner D, Zwick MB, Phogat SK,  
932 Poignard P, Burton DR. 2010. A limited number of antibody specificities mediate  
933 broad and potent serum neutralization in selected HIV-1 infected individuals.  
934 PLoS Pathog 6:e1001028.

935

936 51. Gray ES, Madiga MC, Hermanus T, Moore PL, Wibmer CK, Tumba NL, Werner  
937 L, Mlisana K, Sibeko S, Williamson C, Abdoool Karim SS, Morris L, Team CS.  
938 2011. The neutralization breadth of HIV-1 develops incrementally over four years  
939 and is associated with CD4+ T cell decline and high viral load during acute  
940 infection. J Virol 85:4828-40.

941

942 52. Corti D, Langedijk JP, Hinz A, Seaman MS, Vanzetta F, Fernandez-Rodriguez  
943 BM, Silacci C, Pinna D, Jarrossay D, Balla-Jhagjhoorsingh S, Willems B, Zekveld  
944 MJ, Dreja H, O'Sullivan E, Pade C, Orkin C, Jeffs SA, Montefiori DC, Davis D,  
945 Weissenhorn W, McKnight A, Heeney JL, Sallusto F, Sattentau QJ, Weiss RA,

946 Lanzavecchia A. 2010. Analysis of memory B cell responses and isolation of  
947 novel monoclonal antibodies with neutralizing breadth from HIV-1-infected  
948 individuals. *PLoS One* 5:e8805.

949

950 53. Wu X, Zhou T, Zhu J, Zhang B, Georgiev I, Wang C, Chen X, Longo NS, Louder  
951 M, McKee K, O'Dell S, Perfetto S, Schmidt SD, Shi W, Wu L, Yang Y, Yang ZY,  
952 Yang Z, Zhang Z, Bonsignori M, Crump JA, Kapiga SH, Sam NE, Haynes BF,  
953 Simek M, Burton DR, Koff WC, Doria-Rose NA, Connors M, Program NCS,  
954 Mullikin JC, Nabel GJ, Roederer M, Shapiro L, Kwong PD, Mascola JR. 2011.  
955 Focused evolution of HIV-1 neutralizing antibodies revealed by structures and  
956 deep sequencing. *Science* 333:1593-602.

957

958 54. Hraber P, Seaman MS, Bailer RT, Mascola JR, Montefiori DC, Korber BT. 2014.  
959 Prevalence of broadly neutralizing antibody responses during chronic HIV-1  
960 infection. *AIDS* 28:163-9.

961

962 55. Hessell AJ, Poignard P, Hunter M, Hangartner L, Tehrani DM, Bleeker WK,  
963 Parren PW, Marx PA, Burton DR. 2009. Effective, low-titer antibody protection  
964 against low-dose repeated mucosal SHIV challenge in macaques. *Nat Med*  
965 15:951-4.

966

967 56. Mascola JR, Lewis MG, Stiegler G, Harris D, VanCott TC, Hayes D, Louder MK,  
968 Brown CR, Sapan CV, Frankel SS, Lu Y, Robb ML, Katinger H, Birx DL. 1999.  
969 Protection of macaques against pathogenic simian/human immunodeficiency  
970 virus 89.6PD by passive transfer of neutralizing antibodies. *J Virol* 73:4009-18.

971

972 57. Mascola JR, Stiegler G, VanCott TC, Katinger H, Carpenter CB, Hanson CE,  
973 Beary H, Hayes D, Frankel SS, Birx DL, Lewis MG. 2000. Protection of  
974 macaques against vaginal transmission of a pathogenic HIV-1/SIV chimeric virus  
975 by passive infusion of neutralizing antibodies. *Nat Med* 6:207-10.

976

977 58. Moldt B, Rakasz EG, Schultz N, Chan-Hui PY, Swiderek K, Weisgrau KL,  
978 Piaskowski SM, Bergman Z, Watkins DI, Poignard P, Burton DR. 2012. Highly  
979 potent HIV-specific antibody neutralization in vitro translates into effective  
980 protection against mucosal SHIV challenge in vivo. *Proc Natl Acad Sci U S A*  
981 109:18921-5.

982

983 59. Parren PW, Marx PA, Hessell AJ, Luckay A, Harouse J, Cheng-Mayer C, Moore  
984 JP, Burton DR. 2001. Antibody protects macaques against vaginal challenge with  
985 a pathogenic R5 simian/human immunodeficiency virus at serum levels giving  
986 complete neutralization in vitro. *J Virol* 75:8340-7.

987

988 60. Pauthner MG, Nkolola JP, Havenar-Daughton C, Murrell B, Reiss SM, Bastidas  
989 R, Prevost J, Nedellec R, von Bredow B, Abbink P, Cottrell CA, Kulp DW,  
990 Tokatlian T, Nogal B, Bianchi M, Li H, Lee JH, Butera ST, Evans DT, Hangartner  
991 L, Finzi A, Wilson IA, Wyatt RT, Irvine DJ, Schief WR, Ward AB, Sanders RW,  
992 Crotty S, Shaw GM, Barouch DH, Burton DR. 2019. Vaccine-induced protection

993 from homologous Tier 2 SHIV challenge in nonhuman primates depends on  
994 serum-neutralizing antibody titers. *Immunity* 50:241-52 e6.

995

996 61. Pauthner M, Havenar-Daughton C, Sok D, Nkolola JP, Bastidas R, Boopathy AV,  
997 Carnathan DG, Chandrashekhar A, Cirelli KM, Cottrell CA, Eroshkin AM, Guenaga  
998 J, Kaushik K, Kulp DW, Liu J, McCoy LE, Oom AL, Ozorowski G, Post KW,  
999 Sharma SK, Steichen JM, de Taeye SW, Tokatlian T, Torrents de la Pena A,  
1000 Butera ST, LaBranche CC, Montefiori DC, Silvestri G, Wilson IA, Irvine DJ,  
1001 Sanders RW, Schief WR, Ward AB, Wyatt RT, Barouch DH, Crotty S, Burton DR.  
1002 2017. Elicitation of robust Tier 2 neutralizing antibody responses in nonhuman  
1003 primates by HIV envelope trimer immunization using optimized approaches.  
1004 *Immunity* 46:1073-88 e6.

1005

1006 62. Torrents de la Pena A, de Taeye SW, Sliopen K, LaBranche CC, Burger JA,  
1007 Schermer EE, Montefiori DC, Moore JP, Klasse PJ, Sanders RW. 2018.  
1008 Immunogenicity in rabbits of HIV-1 SOSIP trimers from Clades A, B, and C, given  
1009 individually, sequentially, or in combination. *J Virol* 92:e01957-17.

1010

1011 63. Klasse PJ, LaBranche CC, Ketas TJ, Ozorowski G, Cupo A, Pugach P, Ringe  
1012 RP, Golabek M, van Gils MJ, Guttman M, Lee KK, Wilson IA, Butera ST, Ward  
1013 AB, Montefiori DC, Sanders RW, Moore JP. 2016. Sequential and simultaneous  
1014 immunization of rabbits with HIV-1 envelope glycoprotein SOSIP.664 trimers  
1015 from Clades A, B and C. *PLoS Pathog* 12:e1005864.

1016

1017 64. Hu JK, Crampton JC, Cupo A, Ketas T, van Gils MJ, Sliopen K, de Taeye SW,  
1018 Sok D, Ozorowski G, Deresa I, Stanfield R, Ward AB, Burton DR, Klasse PJ,  
1019 Sanders RW, Moore JP, Crotty S. 2015. Murine antibody responses to cleaved  
1020 soluble HIV-1 envelope trimers are highly restricted in specificity. *J Virol*  
1021 89:10383-98.

1022 .

1023 65. Feng Y, Tran K, Bale S, Kumar S, Guenaga J, Wilson R, de Val N, Arendt H,  
1024 DeStefano J, Ward AB, Wyatt RT. 2016. Thermostability of well-ordered HIV  
1025 spikes correlates with the elicitation of autologous Tier 2 neutralizing antibodies.  
1026 *PLoS Pathog* 12:e1005767.

1027

1028 66. Dubrovskaya V, Tran K, Ozorowski G, Guenaga J, Wilson R, Bale S, Cottrell CA,  
1029 Turner HL, Seabright G, O'Dell S, Torres JL, Yang L, Feng Y, Leaman DP,  
1030 Vazquez Bernat N, Liban T, Louder M, McKee K, Bailer RT, Movsesyan A, Doria-  
1031 Rose NA, Pancera M, Karlsson Hedestam GB, Zwick MB, Crispin M, Mascola  
1032 JR, Ward AB, Wyatt RT. 2019. Vaccination with glycan-modified HIV NFL  
1033 envelope trimer-liposomes elicits broadly neutralizing antibodies to multiple sites  
1034 of vulnerability. *Immunity* 51:915-29 e7.

1035

1036 67. Xu K, Acharya P, Kong R, Cheng C, Chuang GY, Liu K, Louder MK, O'Dell S,  
1037 Rawi R, Sastry M, Shen CH, Zhang B, Zhou T, Asokan M, Bailer RT, Chambers  
1038 M, Chen X, Choi CW, Dandey VP, Doria-Rose NA, Druz A, Eng ET, Farney SK,  
1039 Foulds KE, Geng H, Georgiev IS, Gorman J, Hill KR, Jafari AJ, Kwon YD, Lai YT,

1040 Lemmin T, McKee K, Ohr TY, Ou L, Peng D, Rowshan AP, Sheng Z, Todd JP,  
1041 Tsybovsky Y, Viox EG, Wang Y, Wei H, Yang Y, Zhou AF, Chen R, Yang L,  
1042 Scorpio DG, McDermott AB, Shapiro L, et al. 2018. Epitope-based vaccine  
1043 design yields fusion peptide-directed antibodies that neutralize diverse strains of  
1044 HIV-1. *Nat Med* 24:857-867.

1045

1046 68. Sanders RW, van Gils MJ, Derking R, Sok D, Ketas TJ, Burger JA, Ozorowski G,  
1047 Cupo A, Simonich C, Goo L, Arendt H, Kim HJ, Lee JH, Pugach P, Williams M,  
1048 Debnath G, Moldt B, van Breemen MJ, Isik G, Medina-Ramirez M, Back JW, Koff  
1049 WC, Julien JP, Rakasz EG, Seaman MS, Guttman M, Lee KK, Klasse PJ,  
1050 LaBranche C, Schief WR, Wilson IA, Overbaugh J, Burton DR, Ward AB,  
1051 Montefiori DC, Dean H, Moore JP. 2015. HIV-1 VACCINES. HIV-1 neutralizing  
1052 antibodies induced by native-like envelope trimers. *Science* 349:aac4223.

1053

1054 69. de Taeye SW, Ozorowski G, Torrents de la Pena A, Guttman M, Julien JP, van  
1055 den Kerkhof TL, Burger JA, Pritchard LK, Pugach P, Yasmeen A, Crampton J,  
1056 Hu J, Bontjer I, Torres JL, Arendt H, DeStefano J, Koff WC, Schuitemaker H,  
1057 Eggink D, Berkhout B, Dean H, LaBranche C, Crotty S, Crispin M, Montefiori DC,  
1058 Klasse PJ, Lee KK, Moore JP, Wilson IA, Ward AB, Sanders RW. 2015.  
1059 Immunogenicity of stabilized HIV-1 envelope trimers with reduced exposure of  
1060 non-neutralizing epitopes. *Cell* 163:1702-15.

1061

1062 70. Sanders RW, Derking R, Cupo A, Julien JP, Yasmeen A, de Val N, Kim HJ,  
1063 Blattner C, de la Pena AT, Korzun J, Golabek M, de Los Reyes K, Ketas TJ, van  
1064 Gils MJ, King CR, Wilson IA, Ward AB, Klasse PJ, Moore JP. 2013. A next-  
1065 generation cleaved, soluble HIV-1 Env trimer, BG505 SOSIP.664 gp140,  
1066 expresses multiple epitopes for broadly neutralizing but not non-neutralizing  
1067 antibodies. *PLoS Pathog* 9:e1003618.

1068

1069 71. Alsahafi N, Debbeche O, Sodroski J, Finzi A. 2015. Effects of the I559P gp41  
1070 change on the conformation and function of the human immunodeficiency virus  
1071 (HIV-1) membrane envelope glycoprotein trimer. *PLoS One* 10:e0122111.

1072

1073 72. Alsahafi N, Anand SP, Castillo-Menendez L, Verly MM, Medjahed H, Prevost J,  
1074 Herschhorn A, Richard J, Schon A, Melillo B, Freire E, Smith AB III, Sodroski J,  
1075 Finzi A. 2018. SOSIP Changes Affect Human Immunodeficiency Virus Type 1  
1076 Envelope Glycoprotein Conformation and CD4 Engagement. *J Virol* 92:e01080-  
1077 18.

1078

1079 73. Castillo-Menendez LR, Nguyen HT, Sodroski J. 2019. Conformational  
1080 Differences between Functional Human Immunodeficiency Virus Envelope  
1081 Glycoprotein Trimers and Stabilized Soluble Trimers. *J Virol* 93:e01709-18.

1082

1083 74. Nguyen HT, Alsahafi N, Finzi A, Sodroski JG. 2019. Effects of the SOS  
1084 (A501C/T605C) and DS (I201C/A433C) Disulfide Bonds on HIV-1 Membrane  
1085 Envelope Glycoprotein Conformation and Function. *J Virol* 93:e00304-19.

1086

1087 75. Go EP, Ding H, Zhang S, Ringe RP, Nicely N, Hua D, Steinbock RT, Golabek M,  
1088 Alin J, Alam SM, Cupo A, Haynes BF, Kappes JC, Moore JP, Sodroski JG,  
1089 Desaire H. 2017. Glycosylation benchmark profile for HIV-1 envelope  
1090 glycoprotein production based on eleven Env trimers. *J Virol* 91:e02428-16.  
1091

1092 76. Cao L, Pauthner M, Andrabi R, Rantalainen K, Berndsen Z, Diedrich JK, Menis  
1093 S, Sok D, Bastidas R, Park SR, Delahunty CM, He L, Guenaga J, Wyatt RT,  
1094 Schief WR, Ward AB, Yates JR, 3rd, Burton DR, Paulson JC. 2018. Differential  
1095 processing of HIV envelope glycans on the virus and soluble recombinant trimer.  
1096 *Nat Commun* 9:3693.  
1097

1098 77. Torrents de la Pena A, Rantalainen K, Cottrell CA, Allen JD, van Gils MJ, Torres  
1099 JL, Crispin M, Sanders RW, Ward AB. 2019. Similarities and differences between  
1100 native HIV-1 envelope glycoprotein trimers and stabilized soluble trimer  
1101 mimetics. *PLoS Pathog* 15:e1007920.  
1102

1103 78. Lu M, Ma X, Castillo-Menendez LR, Gorman J, Alsahafi N, Ermel U, Terry DS,  
1104 Chambers M, Peng D, Zhang B, Zhou T, Reichard N, Wang K, Grover JR,  
1105 Carman BP, Gardner MR, Nikic-Spiegel I, Sugawara A, Arthos J, Lemke EA,  
1106 Smith AB III, Farzan M, Abrams C, Munro JB, McDermott AB, Finzi A, Kwong  
1107 PD, Blanchard SC, Sodroski JG, Mothes W. 2019. Associating HIV-1 envelope  
1108 glycoprotein structures with states on the virus observed by smFRET. *Nature*  
1109 568:415-9.  
1110

1111 79. Julien JP, Cupo A, Sok D, Stanfield RL, Lyumkis D, Deller MC, Klasse PJ, Burton  
1112 DR, Sanders RW, Moore JP, Ward AB, Wilson IA. 2013. Crystal structure of a  
1113 soluble cleaved HIV-1 envelope trimer. *Science* 342:1477-83.  
1114

1115 80. Lyumkis D, Julien JP, de Val N, Cupo A, Potter CS, Klasse PJ, Burton DR,  
1116 Sanders RW, Moore JP, Carragher B, Wilson IA, Ward AB. 2013. Cryo-EM  
1117 structure of a fully glycosylated soluble cleaved HIV-1 envelope trimer. *Science*  
1118 342:1484-90.  
1119

1120 81. Pancera M, Zhou T, Druz A, Georgiev IS, Soto C, Gorman J, Huang J, Acharya  
1121 P, Chuang GY, Ofek G, Stewart-Jones GB, Stuckey J, Bailer RT, Joyce MG,  
1122 Louder MK, Tumba N, Yang Y, Zhang B, Cohen MS, Haynes BF, Mascola JR,  
1123 Morris L, Munro JB, Blanchard SC, Mothes W, Connors M, Kwong PD. 2014.  
1124 Structure and immune recognition of trimeric pre-fusion HIV-1 Env. *Nature*  
1125 514:455-61.  
1126

1127 82. Lee JH, Ozorowski G, Ward AB. 2016. Cryo-EM structure of a native, fully  
1128 glycosylated, cleaved HIV-1 envelope trimer. *Science* 351:1043-8.  
1129

1130 83. Bartesaghi A, Merk A, Borgnia MJ, Milne JL, Subramaniam S. 2013. Prefusion  
1131 structure of trimeric HIV-1 envelope glycoprotein determined by cryo-electron  
1132 microscopy. *Nat Struct Mol Biol* 20:1352-7.  
1133

1134 84. Stewart-Jones GB, Soto C, Lemmin T, Chuang GY, Druz A, Kong R, Thomas  
1135 PV, Wagh K, Zhou T, Behrens AJ, Bylund T, Choi CW, Davison JR, Georgiev IS,  
1136 Joyce MG, Kwon YD, Pancera M, Taft J, Yang Y, Zhang B, Shivatare SS,  
1137 Shivatare VS, Lee CC, Wu CY, Bewley CA, Burton DR, Koff WC, Connors M,  
1138 Crispin M, Baxa U, Korber BT, Wong CH, Mascola JR, Kwong PD. 2016.  
1139 Trimeric HIV-1-Env structures define glycan shields from Clades A, B, and G.  
1140 Cell 165:813-26.

1141

1142 85. Gristick HB, von Boehmer L, West AP, Jr., Schamber M, Gazumyan A, Goljanin  
1143 J, Seaman MS, Fatkenheuer G, Klein F, Nussenzweig MC, Bjorkman PJ. 2016.  
1144 Natively glycosylated HIV-1 Env structure reveals new mode for antibody  
1145 recognition of the CD4-binding site. Nat Struct Mol Biol 23:906-915.

1146

1147 86. Kwon YD, Pancera M, Acharya P, Georgiev IS, Crooks ET, Gorman J, Joyce  
1148 MG, Guttman M, Ma X, Narpala S, Soto C, Terry DS, Yang Y, Zhou T, Ahlsen G,  
1149 Bailer RT, Chambers M, Chuang GY, Doria-Rose NA, Druz A, Hallen MA,  
1150 Harned A, Kirys T, Louder MK, O'Dell S, Ofek G, Osawa K, Prabhakaran M,  
1151 Sastry M, Stewart-Jones GB, Stuckey J, Thomas PV, Tittley T, Williams C,  
1152 Zhang B, Zhao H, Zhou Z, Donald BR, Lee LK, Zolla-Pazner S, Baxa U, Schon  
1153 A, Freire E, Shapiro L, Lee KK, Arthos J, Munro JB, Blanchard SC, Mothes W,  
1154 Binley JM, et al. 2015. Crystal structure, conformational fixation and entry-related  
1155 interactions of mature ligand-free HIV-1 Env. Nat Struct Mol Biol 22:522-31.

1156

1157 87. Guenaga J, de Val N, Tran K, Feng Y, Satchwell K, Ward AB, Wyatt RT. 2015.  
1158 Well-ordered trimeric HIV-1 subtype B and C soluble spike mimetics generated  
1159 by negative selection display native-like properties. PLoS Pathog 11:e1004570.

1160

1161 88. Guenaga J, Dubrovskaya V, de Val N, Sharma SK, Carrette B, Ward AB, Wyatt  
1162 RT. 2015. Structure-guided redesign increases the propensity of HIV Env to  
1163 generate highly stable soluble trimers. J Virol 90:2806-17.

1164

1165 89. Georgiev IS, Joyce MG, Yang Y, Sastry M, Zhang B, Baxa U, Chen RE, Druz A,  
1166 Lees CR, Narpala S, Schon A, Van Galen J, Chuang GY, Gorman J, Harned A,  
1167 Pancera M, Stewart-Jones GB, Cheng C, Freire E, McDermott AB, Mascola JR,  
1168 Kwong PD. 2015. Single-chain soluble BG505.SOSIP gp140 trimers as structural  
1169 and antigenic mimics of mature closed HIV-1 Env. J Virol 89:5318-29.

1170

1171 90. Yang Z, Wang H, Liu AZ, Gristick HB, Bjorkman PJ. 2019. Asymmetric opening  
1172 of HIV-1 Env bound to CD4 and a coreceptor-mimicking antibody. Nat Struct Mol  
1173 Biol 26:1167-1175.

1174

1175 91. Pan J, Peng H, Chen B, Harrison SC. 2020. Cryo-EM structure of full-length HIV-  
1176 1 Env bound with the Fab of antibody PG16. J Mol Biol 432:1158-1168.

1177

1178 92. Roberts JD, Bebenek K, Kunkel TA. 1988. The accuracy of reverse transcriptase  
1179 from HIV-1. Science 242:1171-3.

1180

1181 93. Smyth RP, Davenport MP, Mak J. 2012. The origin of genetic diversity in HIV-1.  
1182 Virus Res 169:415-29.

1183

1184 94. Cuevas JM, Geller R, Garijo R, Lopez-Aldeguer J, Sanjuan R. 2015. Extremely  
1185 high mutation rate of HIV-1 in vivo. PLoS Biol 13:e1002251.

1186

1187 95. Monajemi M, Woodworth CF, Zipperlen K, Gallant M, Grant MD, Larijani M.  
1188 2014. Positioning of APOBEC3G/F mutational hotspots in the human  
1189 immunodeficiency virus genome favors reduced recognition by CD8+ T cells.  
1190 PLoS One 9:e93428.

1191

1192 96. Sadler HA, Stenglein MD, Harris RS, Mansky LM. 2010. APOBEC3G contributes  
1193 to HIV-1 variation through sublethal mutagenesis. J Virol 84:7396-404.

1194

1195 97. Mansky LM, Le Rouzic E, Benichou S, Gajary LC. 2003. Influence of reverse  
1196 transcriptase variants, drugs, and Vpr on human immunodeficiency virus type 1  
1197 mutant frequencies. J Virol 77:2071-80.

1198

1199 98. Fraser C, Lythgoe K, Leventhal GE, Shirreff G, Hollingsworth TD, Alizon S,  
1200 Bonhoeffer S. 2014. Virulence and pathogenesis of HIV-1 infection: an  
1201 evolutionary perspective. Science 343:1243727.

1202

1203 99. Davenport MP, Loh L, Petracic J, Kent SJ. 2008. Rates of HIV immune escape  
1204 and reversion: implications for vaccination. Trends Microbiol 16:561-6.

1205

1206 100. Hraber P, Korber BT, Lapedes AS, Bailer RT, Seaman MS, Gao H, Greene KM,  
1207 McCutchan F, Williamson C, Kim JH, Tovanabutra S, Hahn BH, Swanson R,  
1208 Thomson MM, Gao F, Harris L, Giorgi E, Hengartner N, Bhattacharya T, Mascola  
1209 JR, Montefiori DC. 2014. Impact of clade, geography, and age of the epidemic on  
1210 HIV-1 neutralization by antibodies. J Virol 88:12623-43.

1211

1212 101. Kolchinsky P, Mirzabekov T, Farzan M, Kiprilov E, Cayabyab M, Mooney LJ,  
1213 Choe H, Sodroski J. 1999. Adaptation of a CCR5-using, primary human  
1214 immunodeficiency virus type 1 isolate for CD4-independent replication. J Virol  
1215 73:8120-6.

1216

1217 102. Hoffman TL, LaBranche CC, Zhang W, Canziani G, Robinson J, Chaiken I, Hoxie  
1218 JA, Doms RW. 1999. Stable exposure of the coreceptor-binding site in a CD4-  
1219 independent HIV-1 envelope protein. Proc Natl Acad Sci U S A 96:6359-64.

1220

1221 103. Dumonceaux J, Nisole S, Chanel C, Quivet L, Amara A, Baleux F, Briand P,  
1222 Hazan U. 1998. Spontaneous mutations in the env gene of the human  
1223 immunodeficiency virus type 1 NDK isolate are associated with a CD4-  
1224 independent entry phenotype. J Virol 72:512-9.

1225

1226 104. Taylor BM, Foulke JS, Flinko R, Heredia A, DeVico A, Reitz M. 2008. An  
1227 alteration of human immunodeficiency virus gp41 leads to reduced CCR5

1228 dependence and CD4 independence. *J Virol* 82:5460-71.

1229

1230 105. Beauparlant D, Rusert P, Magnus C, Kadelka C, Weber J, Uhr T, Zagordi O,  
1231 Oberle C, Duenas-Decamp MJ, Clapham PR, Metzner KJ, Gunthard HF, Trkola  
1232 A. 2017. Delineating CD4 dependency of HIV-1: Adaptation to infect low level  
1233 CD4 expressing target cells widens cellular tropism but severely impacts on  
1234 envelope functionality. *PLoS Pathog* 13:e1006255.

1235

1236 106. Zerhouni B, Nelson JA, Saha K. 2004. Isolation of CD4-independent primary  
1237 human immunodeficiency virus type 1 isolates that are syncytium inducing and  
1238 acutely cytopathic for CD8+ lymphocytes. *J Virol* 78:1243-55.

1239

1240 107. Bhattacharya J, Peters PJ, Clapham PR. 2003. CD4-independent infection of  
1241 HIV and SIV: implications for envelope conformation and cell tropism in vivo.  
1242 *AIDS* 17 Suppl 4:S35-43.

1243

1244 108. LaBranche CC, Hoffman TL, Romano J, Haggarty BS, Edwards TG, Matthews  
1245 TJ, Doms RW, Hoxie JA. 1999. Determinants of CD4 independence for a human  
1246 immunodeficiency virus type 1 variant map outside regions required for  
1247 coreceptor specificity. *J Virol* 73:10310-9.

1248

1249 109. Edwards TG, Wyss S, Reeves JD, Zolla-Pazner S, Hoxie JA, Doms RW,  
1250 Baribaud F. 2002. Truncation of the cytoplasmic domain induces exposure of  
1251 conserved regions in the ectodomain of human immunodeficiency virus type 1  
1252 envelope protein. *J Virol* 76:2683-91.

1253

1254 110. Kolchinsky P, Kiprilov E, Sodroski J. 2001. Increased neutralization sensitivity of  
1255 CD4-independent human immunodeficiency virus variants. *J Virol* 75:2041-50.

1256

1257 111. Shin Y, Yoon CH, Yang HJ, Lim H, Choi BS, Kim SS, Kang C. 2016. Functional  
1258 characteristics of the natural polymorphisms of HIV-1 gp41 in HIV-1 isolates from  
1259 enfuvirtide-naive Korean patients. *Arch Virol* 161:1547-57.

1260

1261 112. Carmona R, Perez-Alvarez L, Munoz M, Casado G, Delgado E, Sierra M,  
1262 Thomson M, Vega Y, Vazquez de Parga E, Contreras G, Medrano L, Najera R.  
1263 2005. Natural resistance-associated mutations to Enfuvirtide (T20) and  
1264 polymorphisms in the gp41 region of different HIV-1 genetic forms from T20  
1265 naive patients. *J Clin Virol* 32:248-53.

1266

1267 113. Moyo T, Ereno-Orbea J, Jacob RA, Pavillet CE, Kariuki SM, Tangie EN, Julien  
1268 JP, Dorfman JR. 2018. Molecular basis of unusually high neutralization  
1269 resistance in Tier 3 HIV-1 strain 253-11. *J Virol* 92:e02261-17.

1270

1271 114. Zhang PF, Bouma P, Park EJ, Margolick JB, Robinson JE, Zolla-Pazner S, Flora  
1272 MN, Quinnan GV, Jr. 2002. A variable region 3 (V3) mutation determines a global  
1273 neutralization phenotype and CD4-independent infectivity of a human  
1274 immunodeficiency virus type 1 envelope associated with a broadly cross-

1275 reactive, primary virus-neutralizing antibody response. *J Virol* 76:644-55.

1276

1277 115. Zolla-Pazner S, Cohen SS, Boyd D, Kong XP, Seaman M, Nussenzweig M, Klein  
1278 F, Overbaugh J, Totrov M. 2016. Structure/function studies involving the V3  
1279 region of the HIV-1 envelope delineate multiple factors that affect neutralization  
1280 sensitivity. *J Virol* 90:636-49.

1281

1282 116. Powell RLR, Totrov M, Itri V, Liu X, Fox A, Zolla-Pazner S. 2017. Plasticity and  
1283 epitope exposure of the HIV-1 envelope trimer. *J Virol* 91.

1284

1285 117. Bradley T, Trama A, Tumba N, Gray E, Lu X, Madani N, Jahanbakhsh F, Eaton  
1286 A, Xia SM, Parks R, Lloyd KE, Sutherland LL, Scearce RM, Bowman CM,  
1287 Barnett S, Abdoool-Karim SS, Boyd SD, Melillo B, Smith AB III, Sodroski J, Kepler  
1288 TB, Alam SM, Gao F, Bonsignori M, Liao HX, Moody MA, Montefiori D, Santra S,  
1289 Morris L, Haynes BF. 2016. Amino acid changes in the HIV-1 gp41 membrane  
1290 proximal region control virus neutralization sensitivity. *EBioMedicine* 12:196-207.

1291

1292 118. Herschhorn A, Gu C, Moraca F, Ma X, Farrell M, Smith AB III, Pancera M,  
1293 Kwong PD, Schon A, Freire E, Abrams C, Blanchard SC, Mothes W, Sodroski  
1294 JG. 2017. The beta20-beta21 of gp120 is a regulatory switch for HIV-1 Env  
1295 conformational transitions. *Nat Commun* 8:1049.

1296

1297 119. Guzzo C, Zhang P, Liu Q, Kwon AL, Uddin F, Wells AI, Schmeisser H, Cimbro R,  
1298 Huang J, Doria-Rose N, Schmidt SD, Dolan MA, Connors M, Mascola JR, Lusso  
1299 P. 2018. Structural constraints at the trimer apex stabilize the HIV-1 envelope in  
1300 a closed, antibody-protected conformation. *mBio* 9:e00955-18.

1301

1302 120. McGee K, Haim H, Korioth-Schmitz B, Espy N, Javanbakht H, Letvin N, Sodroski  
1303 J. 2014. The selection of low envelope glycoprotein reactivity to soluble CD4 and  
1304 cold during simian-human immunodeficiency virus infection of rhesus macaques.  
1305 *J Virol* 88:21-40.

1306

1307 121. Kassa A, Finzi A, Pancera M, Courter JR, Smith AB III, Sodroski J. 2009.  
1308 Identification of a human immunodeficiency virus type 1 envelope glycoprotein  
1309 variant resistant to cold inactivation. *J Virol* 83:4476-88.

1310

1311 122. Kassa A, Madani N, Schon A, Haim H, Finzi A, Xiang SH, Wang L, Princiotto A,  
1312 Pancera M, Courter J, Smith AB III, Freire E, Kwong PD, Sodroski J. 2009.  
1313 Transitions to and from the CD4-bound conformation are modulated by a single-  
1314 residue change in the human immunodeficiency virus type 1 gp120 inner domain.  
1315 *J Virol* 83:8364-78.

1316

1317 123. Klasse PJ, McKeating JA, Schutten M, Reitz MS, Jr., Robert-Guroff M. 1993. An  
1318 immune-selected point mutation in the transmembrane protein of human  
1319 immunodeficiency virus type 1 (HXB2-Env:Ala 582-->Thr)) decreases viral  
1320 neutralization by monoclonal antibodies to the CD4-binding site. *Virology*  
1321 196:332-7.

1322  
1323 124. Thali M, Charles M, Furman C, Cavacini L, Posner M, Robinson J, Sodroski J.  
1324 1994. Resistance to neutralization by broadly reactive antibodies to the human  
1325 immunodeficiency virus type 1 gp120 glycoprotein conferred by a gp41 amino  
1326 acid change. *J Virol* 68:674-80.

1327  
1328 125. Pacheco B, Alsahafi N, Debbeche O, Prevost J, Ding S, Chapleau JP,  
1329 Herschhorn A, Madani N, Princiotto A, Melillo B, Gu C, Zeng X, Mao Y, Smith AB  
1330 III, Sodroski J, Finzi A. 2017. Residues in the gp41 ectodomain regulate HIV-1  
1331 envelope glycoprotein conformational transitions induced by gp120-directed  
1332 inhibitors. *J Virol* 91:e02219-16.

1333  
1334 126. Schiffner T, Pallesen J, Russell RA, Dodd J, de Val N, LaBranche CC, Montefiori  
1335 D, Tomaras GD, Shen X, Harris SL, Moghaddam AE, Kalyuzhniy O, Sanders  
1336 RW, McCoy LE, Moore JP, Ward AB, Sattentau QJ. 2018. Structural and  
1337 immunologic correlates of chemically stabilized HIV-1 envelope glycoproteins.  
1338 *PLoS Pathog* 14:e1006986.

1339  
1340 127. Shen X, Bogers WM, Yates NL, Ferrari G, Dey AK, Williams WT, Jaeger FH,  
1341 Wiehe K, Sawant S, Alam SM, LaBranche CC, Montefiori DC, Martin L,  
1342 Srivastava I, Heeney J, Barnett SW, Tomaras GD. 2017. Cross-linking of a CD4-  
1343 mimetic miniprotein with HIV-1 Env gp140 alters kinetics and specificities of  
1344 antibody responses against HIV-1 Env in macaques. *J Virol* 91:e00401-17.

1345  
1346 128. Schiffner T, de Val N, Russell RA, de Taeye SW, de la Pena AT, Ozorowski G,  
1347 Kim HJ, Nieuwsma T, Brod F, Cupo A, Sanders RW, Moore JP, Ward AB,  
1348 Sattentau QJ. 2016. Chemical cross-linking stabilizes native-like HIV-1 envelope  
1349 glycoprotein trimer antigens. *J Virol* 90:813-28.

1350  
1351 129. Schiffner T, Kong L, Duncan CJ, Back JW, Benschop JJ, Shen X, Huang PS,  
1352 Stewart-Jones GB, DeStefano J, Seaman MS, Tomaras GD, Montefiori DC,  
1353 Schief WR, Sattentau QJ. 2013. Immune focusing and enhanced neutralization  
1354 induced by HIV-1 gp140 chemical cross-linking. *J Virol* 87:10163-72.

1355  
1356 130. Yuan W, Bazick J, Sodroski J. 2006. Characterization of the multiple  
1357 conformational States of free monomeric and trimeric human immunodeficiency  
1358 virus envelope glycoproteins after fixation by cross-linker. *J Virol* 80:6725-37.

1359  
1360 131. Witt KC, Castillo-Menendez L, Ding H, Espy N, Zhang S, Kappes JC, Sodroski J.  
1361 2017. Antigenic characterization of the human immunodeficiency virus (HIV-1)  
1362 envelope glycoprotein precursor incorporated into nanodiscs. *PLoS One*  
1363 12:e0170672.

1364  
1365 132. Leitner A, Walzthoeni T, Aebersold R. 2014. Lysine-specific chemical cross-  
1366 linking of protein complexes and identification of cross-linking sites using LC-  
1367 MS/MS and the xQuest/xProphet software pipeline. *Nat Protoc* 9:120-37.

1368

1369 133. Merkley ED, Rysavy S, Kahraman A, Hafen RP, Daggett V, Adkins JN. 2014.  
1370 Distance restraints from crosslinking mass spectrometry: mining a molecular  
1371 dynamics simulation database to evaluate lysine-lysine distances. *Protein Sci*  
1372 23:747-59.

1373

1374 134. Singh P, Panchaud A, Goodlett DR. 2010. Chemical cross-linking and mass  
1375 spectrometry as a low-resolution protein structure determination technique. *Anal*  
1376 *Chem* 82:2636-42.

1377

1378 135. Leitner A, Joachimiak LA, Unverdorben P, Walzthoeni T, Frydman J, Forster F,  
1379 Aebersold R. 2014. Chemical cross-linking/mass spectrometry targeting acidic  
1380 residues in proteins and protein complexes. *Proc Natl Acad Sci U S A* 111:9455-  
1381 60.

1382

1383 136. Foley B, Leitner T, Apetrei C, Hahn B, Mizrahi I, Mullins J, Rambaut A, Wolinsky  
1384 S, Korber B, eds. 2014. HIV sequence compendium 2014. Los Alamos National  
1385 Laboratory, Theoretical Biology and Biophysics, Los Alamos, New Mexico. LA-  
1386 UR-14-26717.

1387

1388 137. Moore JP, Trkola A, Korber B, Boots LJ, Kessler JA, 2nd, McCutchan FE,  
1389 Mascola J, Ho DD, Robinson J, Conley AJ. 1995. A human monoclonal antibody  
1390 to a complex epitope in the V3 region of gp120 of human immunodeficiency virus  
1391 type 1 has broad reactivity within and outside clade B. *J Virol* 69:122-30.

1392

1393 138. Zou S, Zhang S, Gaffney A, Ding H, Lu M, Grover JR, Farrell M, Nguyen HT,  
1394 Zhao C, Anang S, Zhao M, Mohammadi M, Blanchard SC, Abrams C, Madani N,  
1395 Mothes W, Kappes JC, Smith AB III, Sodroski J. 2020. Long-acting BMS-378806  
1396 analogues stabilize the State-1 conformation of the human immunodeficiency  
1397 virus type 1 envelope glycoproteins. *J Virol* 94:e00148-20.

1398

1399 139. Lu M, Ma X, Reichard N, Terry DS, Arthos J, Smith AB III, Sodroski JG,  
1400 Blanchard SC, Mothes W. 2020. Shedding-resistant HIV-1 envelope  
1401 glycoproteins adopt downstream conformations that remain responsive to  
1402 conformation-preferring ligands. *J Virol* 94:e00597-20.

1403

1404 140. Si Z, Madani N, Cox JM, Chruma JJ, Klein JC, Schon A, Phan N, Wang L, Biorn  
1405 AC, Cocklin S, Chaiken I, Freire E, Smith AB III, Sodroski JG. 2004. Small-  
1406 molecule inhibitors of HIV-1 entry block receptor-induced conformational  
1407 changes in the viral envelope glycoproteins. *Proc Natl Acad Sci U S A* 101:5036-  
1408 41.

1409

1410 141. Moore JP, McKeating JA, Weiss RA, Sattentau QJ. 1990. Dissociation of gp120  
1411 from HIV-1 virions induced by soluble CD4. *Science* 250:1139-42.

1412

1413 142. McKeating JA, McKnight A, Moore JP. 1991. Differential loss of envelope  
1414 glycoprotein gp120 from virions of human immunodeficiency virus type 1 isolates:  
1415 effects on infectivity and neutralization. *J Virol* 65:852-60.

1416

1417 143. Li Y, O'Dell S, Walker LM, Wu X, Guenaga J, Feng Y, Schmidt SD, McKee K,  
1418 Louder MK, Ledgerwood JE, Graham BS, Haynes BF, Burton DR, Wyatt RT,  
1419 Mascola JR. 2011. Mechanism of neutralization by the broadly neutralizing HIV-1  
1420 monoclonal antibody VRC01. *J Virol* 85:8954-67.

1421

1422 144. Wu X, Yang ZY, Li Y, Hogerkorp CM, Schief WR, Seaman MS, Zhou T, Schmidt  
1423 SD, Wu L, Xu L, Longo NS, McKee K, O'Dell S, Louder MK, Wycuff DL, Feng Y,  
1424 Nason M, Doria-Rose N, Connors M, Kwong PD, Roederer M, Wyatt RT, Nabel  
1425 GJ, Mascola JR. 2010. Rational design of envelope identifies broadly neutralizing  
1426 human monoclonal antibodies to HIV-1. *Science* 329:856-61.

1427

1428 145. Pancera M, Shahzad-Ui-Hussan S, Doria-Rose NA, McLellan JS, Bailer RT, Dai  
1429 K, Loesgen S, Louder MK, Staupe RP, Yang Y, Zhang B, Parks R, Eudailey J,  
1430 Lloyd KE, Blinn J, Alam SM, Haynes BF, Amin MN, Wang LX, Burton DR, Koff  
1431 WC, Nabel GJ, Mascola JR, Bewley CA, Kwong PD. 2013. Structural basis for  
1432 diverse N-glycan recognition by HIV-1-neutralizing V1-V2-directed antibody  
1433 PG16. *Nat Struct Mol Biol* 20:804-13.

1434

1435 146. Julien JP, Sok D, Khayat R, Lee JH, Doores KJ, Walker LM, Ramos A, Diwanji  
1436 DC, Pejchal R, Cupo A, Katpally U, Depetris RS, Stanfield RL, McBride R,  
1437 Marozsan AJ, Paulson JC, Sanders RW, Moore JP, Burton DR, Poignard P,  
1438 Ward AB, Wilson IA. 2013. Broadly neutralizing antibody PGT121 allosterically  
1439 modulates CD4 binding via recognition of the HIV-1 gp120 V3 base and multiple  
1440 surrounding glycans. *PLoS Pathog* 9:e1003342.

1441

1442 147. Huang J, Kang BH, Pancera M, Lee JH, Tong T, Feng Y, Imamichi H, Georgiev  
1443 IS, Chuang GY, Druz A, Doria-Rose NA, Laub L, Sliepen K, van Gils MJ, de la  
1444 Pena AT, Derking R, Klasse PJ, Migueles SA, Bailer RT, Alam M, Pugach P,  
1445 Haynes BF, Wyatt RT, Sanders RW, Binley JM, Ward AB, Mascola JR, Kwong  
1446 PD, Connors M. 2014. Broad and potent HIV-1 neutralization by a human  
1447 antibody that binds the gp41-gp120 interface. *Nature* 515:138-42.

1448

1449 148. Thali M, Moore JP, Furman C, Charles M, Ho DD, Robinson J, Sodroski J. 1993.  
1450 Characterization of conserved human immunodeficiency virus type 1 gp120  
1451 neutralization epitopes exposed upon gp120-CD4 binding. *J Virol* 67:3978-88.

1452

1453 149. Madani N, Princiotto AM, Easterhoff D, Bradley T, Luo K, Williams WB, Liao HX,  
1454 Moody MA, Phad GE, Vazquez Bernat N, Melillo B, Santra S, Smith AB III,  
1455 Karlsson Hedestam GB, Haynes B, Sodroski J. 2016. Antibodies elicited by  
1456 multiple envelope glycoprotein immunogens in primates neutralize primary  
1457 human immunodeficiency viruses (HIV-1) sensitized by CD4-mimetic  
1458 compounds. *J Virol* 90:5031-5046.

1459

1460 150. Posner MR, Hidemitsu T, Cannon T, Mukherjee M, Mayer KH, Byrn RA. 1991.  
1461 An IgG human monoclonal antibody that reacts with HIV-1/GP120, inhibits virus  
1462 binding to cells, and neutralizes infection. *J Immunol* 146:4325-32.

1463  
1464 151. Melillo B, Liang S, Park J, Schon A, Courter JR, LaLonde JM, Wendler DJ,  
1465 Princiotto AM, Seaman MS, Freire E, Sodroski J, Madani N, Hendrickson WA,  
1466 Smith AB III. 2016. Small-molecule CD4-mimics: Structure-based optimization of  
1467 HIV-1 entry inhibition. *ACS Med Chem Lett* 7:330-4.

1468  
1469 152. Kwong PD, Wyatt R, Robinson J, Sweet RW, Sodroski J, Hendrickson WA. 1998.  
1470 Structure of an HIV gp120 envelope glycoprotein in complex with the CD4  
1471 receptor and a neutralizing human antibody. *Nature* 393:648-59.

1472  
1473 153. Wyatt R, Kwong PD, Desjardins E, Sweet RW, Robinson J, Hendrickson WA,  
1474 Sodroski JG. 1998. The antigenic structure of the HIV gp120 envelope  
1475 glycoprotein. *Nature* 393:705-11.

1476  
1477 154. Finzi A, Xiang SH, Pacheco B, Wang L, Haight J, Kassa A, Danek B, Pancera M,  
1478 Kwong PD, Sodroski J. 2010. Topological layers in the HIV-1 gp120 inner  
1479 domain regulate gp41 interaction and CD4-triggered conformational transitions.  
1480 *Mol Cell* 37:656-67.

1481  
1482 155. Pancera M, Majeed S, Ban YE, Chen L, Huang CC, Kong L, Kwon YD, Stuckey  
1483 J, Zhou T, Robinson JE, Schief WR, Sodroski J, Wyatt R, Kwong PD. 2010.  
1484 Structure of HIV-1 gp120 with gp41-interactive region reveals layered envelope  
1485 architecture and basis of conformational mobility. *Proc Natl Acad Sci U S A*  
1486 107:1166-71.

1487  
1488 156. Mao Y, Wang L, Gu C, Herschhorn A, Desormeaux A, Finzi A, Xiang SH,  
1489 Sodroski JG. 2013. Molecular architecture of the uncleaved HIV-1 envelope  
1490 glycoprotein trimer. *Proc Natl Acad Sci U S A* 110:12438-43.

1491  
1492 157. Blattner C, Lee JH, Sliepen K, Derking R, Falkowska E, de la Pena AT, Cupo A,  
1493 Julien JP, van Gils M, Lee PS, Peng W, Paulson JC, Poignard P, Burton DR,  
1494 Moore JP, Sanders RW, Wilson IA, Ward AB. 2014. Structural delineation of a  
1495 quaternary, cleavage-dependent epitope at the gp41-gp120 interface on intact  
1496 HIV-1 Env trimers. *Immunity* 40:669-80.

1497  
1498 158. Walker LM, Huber M, Doores KJ, Falkowska E, Pejchal R, Julien JP, Wang SK,  
1499 Ramos A, Chan-Hui PY, Moyle M, Mitcham JL, Hammond PW, Olsen OA, Phung  
1500 P, Fling S, Wong CH, Phogat S, Wrin T, Simek MD, Protocol GPI, Koff WC,  
1501 Wilson IA, Burton DR, Poignard P. 2011. Broad neutralization coverage of HIV by  
1502 multiple highly potent antibodies. *Nature* 477:466-70.

1503  
1504 159. Cavacini LA, Emes CL, Wisnewski AV, Power J, Lewis G, Montefiori D, Posner  
1505 MR. 1998. Functional and molecular characterization of human monoclonal  
1506 antibody reactive with the immunodominant region of HIV type 1 glycoprotein 41.  
1507 *AIDS Res Hum Retroviruses* 14:1271-80.

1508  
1509 160. Chaiken I, Rashad AA. 2015. Peptide triazole inactivators of HIV-1: how do they

1510 work and what is their potential? Future Med Chem 7:2305-10.

1511

1512 161. Labrosse B, Treboute C, Alizon M. 2000. Sensitivity to a nonpeptidic compound  
1513 (RPR103611) blocking human immunodeficiency virus type 1 Env-mediated  
1514 fusion depends on sequence and accessibility of the gp41 loop region. J Virol  
1515 74:2142-50.

1516

1517 162. Madani N, Schon A, Princiotto AM, Lalonde JM, Courter JR, Soeta T, Ng D,  
1518 Wang L, Brower ET, Xiang SH, Kwon YD, Huang CC, Wyatt R, Kwong PD,  
1519 Freire E, Smith AB III, Sodroski J. 2008. Small-molecule CD4 mimics interact  
1520 with a highly conserved pocket on HIV-1 gp120. Structure 16:1689-701.

1521

1522 163. Migneault I, Dartiguenave C, Bertrand MJ, Waldron KC. 2004. Glutaraldehyde:  
1523 behavior in aqueous solution, reaction with proteins, and application to enzyme  
1524 crosslinking. BioTechniques 37:790-802.

1525

1526 164. Privalov PL. 1990. Cold denaturation of proteins. Crit Rev Biochem Mol Biol  
1527 25:281-305.

1528

1529 165. Tsai CJ, Maizel JV, Jr., Nussinov R. 2002. The hydrophobic effect: a new insight  
1530 from cold denaturation and a two-state water structure. Crit Rev Biochem Mol  
1531 Biol 37:55-69.

1532

1533 166. Lopez CF, Darst RK, Rossky PJ. 2008. Mechanistic elements of protein cold  
1534 denaturation. J Phys Chem B 112:5961-7.

1535

1536 167. Herrera C, Klasse PJ, Michael E, Kake S, Barnes K, Kibler CW, Campbell-  
1537 Gardener L, Si Z, Sodroski J, Moore JP, Beddows S. 2005. The impact of  
1538 envelope glycoprotein cleavage on the antigenicity, infectivity, and neutralization  
1539 sensitivity of Env-pseudotyped human immunodeficiency virus type 1 particles.  
1540 Virology 338:154-72.

1541

1542 168. Pancera M, Wyatt R. 2005. Selective recognition of oligomeric HIV-1 primary  
1543 isolate envelope glycoproteins by potently neutralizing ligands requires efficient  
1544 precursor cleavage. Virology 332:145-56.

1545

1546 169. Chakrabarti BK, Pancera M, Phogat S, O'Dell S, McKee K, Guenaga J, Robinson  
1547 J, Mascola J, Wyatt RT. 2011. HIV type 1 Env precursor cleavage state affects  
1548 recognition by both neutralizing and nonneutralizing gp41 antibodies. AIDS Res  
1549 Hum Retroviruses 27:877-87.

1550

1551 170. Chakrabarti BK, Walker LM, Guenaga JF, Ghobbeh A, Poignard P, Burton DR,  
1552 Wyatt RT. 2011. Direct antibody access to the HIV-1 membrane-proximal  
1553 external region positively correlates with neutralization sensitivity. J Virol  
1554 85:8217-26.

1555

1556 171. Li Y, O'Dell S, Wilson R, Wu X, Schmidt SD, Hogerkorp CM, Louder MK, Longo

1557 NS, Poulsen C, Guenaga J, Chakrabarti BK, Doria-Rose N, Roederer M,  
1558 Connors M, Mascola JR, Wyatt RT. 2012. HIV-1 neutralizing antibodies display  
1559 dual recognition of the primary and coreceptor binding sites and preferential  
1560 binding to fully cleaved envelope glycoproteins. *J Virol* 86:11231-41.

1561

1562 172. Haim H, Salas I, Sodroski J. 2013. Proteolytic processing of the human  
1563 immunodeficiency virus envelope glycoprotein precursor decreases  
1564 conformational flexibility. *J Virol* 87:1884-9.

1565

1566 173. Castillo-Menendez LR, Witt K, Espy N, Princiotto A, Madani N, Pacheco B, Finzi  
1567 A, Sodroski J. 2018. Comparison of uncleaved and mature human  
1568 immunodeficiency virus membrane envelope glycoprotein trimers. *J Virol*  
1569 92:e00277-18.

1570

1571 174. Gift SK, Leaman DP, Zhang L, Kim AS, Zwick MB. 2017. Functional stability of  
1572 HIV-1 envelope trimer affects accessibility to broadly neutralizing antibodies at its  
1573 apex. *J Virol* 91:e01216-17.

1574

1575 175. Dey AK, David KB, Klasse PJ, Moore JP. 2007. Specific amino acids in the N-  
1576 terminus of the gp41 ectodomain contribute to the stabilization of a soluble,  
1577 cleaved gp140 envelope glycoprotein from human immunodeficiency virus type  
1578 1. *Virology* 360:199-208.

1579

1580 176. Dey AK, David KB, Ray N, Ketas TJ, Klasse PJ, Doms RW, Moore JP. 2008. N-  
1581 terminal substitutions in HIV-1 gp41 reduce the expression of non-trimeric  
1582 envelope glycoproteins on the virus. *Virology* 372:187-200.

1583

1584 177. Sanders RW, Vesananen M, Schuelke N, Master A, Schiffner L, Kalyanaraman R,  
1585 Paluch M, Berkhout B, Maddon PJ, Olson WC, Lu M, Moore JP. 2002.  
1586 Stabilization of the soluble, cleaved, trimeric form of the envelope glycoprotein  
1587 complex of human immunodeficiency virus type 1. *J Virol* 76:8875-89.

1588

1589 178. Wang Q, Liu L, Ren W, Gettie A, Wang H, Liang Q, Shi X, Montefiori DC, Zhou  
1590 T, Zhang L. 2019. A single substitution in gp41 modulates the neutralization  
1591 profile of SHIV during in vivo adaptation. *Cell Rep* 27:2593-2607 e5.

1592

1593

1594 **TABLE LEGENDS**

1595 **Table 1. Phenotypes of HIV-1<sub>AD8</sub> Env variants with changes in Gln 114 and Gln**  
1596 **567.**

1597 The phenotypes of the wild-type HIV-1<sub>AD8</sub> Env and the indicated Gln 114 and Gln 567  
1598 variants were determined as in Figure 2. The values for Env processing efficiency, virus  
1599 infectivity and gp120-trimer association, relative to those observed for the wild-type HIV-  
1600 1<sub>AD8</sub> Env, are shown. The sensitivity or resistance of viruses with the Env variants to  
1601 cold, sCD4 and BNM-III-170 is reported relative to that of the wild-type HIV-1<sub>AD8</sub> virus.  
1602 To ensure accurate comparison of the Env variant phenotypes across multiple assays,  
1603 the wild-type HIV-1<sub>AD8</sub> and key Env mutants (e.g., Q114E or Q567K) were included in all  
1604 assays. Phenotypes are labelled as follows: •, wild-type level; +, increase; -, decrease;  
1605 R, resistant; S, sensitive; ND, not determined; NA, not applicable. For virus infectivity:  
1606 0-25 % of wild-type, - - -; 25-50 %, - -; 50-75 %, -; 75-125 %, •; >125 %, +. The data  
1607 shown are representative of results obtained in at least two independent experiments.

1608

1609 **Table 2. Effects of Env amino acid changes on the phenotypes of the Q114E and**  
1610 **Q567K Env variants.**

1611 The phenotypes of the wild-type and mutant HIV-1<sub>AD8</sub> Envs were determined as in  
1612 Figure 2. The values, relative to those of the wild-type HIV-1<sub>AD8</sub> Env, are reported as  
1613 described in the legend to Table 1. The data shown are representative of results  
1614 obtained in at least two independent experiments.

1615

1616 **Table 3. Effects of Env amino acid changes on the phenotypes of the E.2, AE.2**  
1617 **and 2-4 RM6 AE Env variants.**

1618 The indicated amino acid changes were introduced into the HIV-1<sub>AD8</sub> Env or into the  
1619 E.2, AE.2 or 2-4 RM6 AE Envs. The phenotypes of these Env variants were determined  
1620 as in Figure 2. The values, relative to those of the wild-type HIV-1<sub>AD8</sub> Env, are reported  
1621 as described in the Table 1 legend. The data shown are representative of results  
1622 obtained in at least two independent experiments.

1623 \*Val 255 is near the binding site for sCD4 and the CD4-mimetic compounds; therefore,  
1624 the V255I change may directly decrease the binding of these Env ligands.

1625

1626

1627 **FIGURE LEGENDS**

1628 **Figure 1. HIV-1<sub>AD8</sub> Env modification guided by natural polymorphisms. (A)**

1629 Natural polymorphisms in HIV-1 Env were used to suggest amino acid residues that  
1630 might tolerate replacement with a lysine residue or with acidic amino acid residues. The  
1631 lysine substitutions are grouped according to the Env region in which the residues are  
1632 located. Compared with Sets 1-3, Sets 4-7 contain an increased number of  
1633 substitutions. (B) A schematic representation of the HIV-1<sub>AD8</sub> Env glycoprotein is  
1634 shown, with the gp120-gp41 cleavage site depicted as a black triangle. S, signal  
1635 peptide; V1-V5, gp120 major hypervariable regions; FP, fusion peptide; HR, heptad  
1636 repeat region; TM, transmembrane region; CT, cytoplasmic tail. The amino acid  
1637 changes associated with some of the key Env variants studied here are shown. Red  
1638 vertical tick marks indicate changes in addition to those found in the 2-4 R Env.

1639

1640 **Figure 2. Phenotypes of the 2-4 R and 2-4 RED2 Envs. (A)** HOS cells were  
1641 transfected transiently with plasmids expressing His<sub>6</sub>-tagged wild-type HIV-1<sub>AD8</sub> Env or  
1642 the 2-4 R or 2-4 RED2 Env variants. Forty-eight hours later, cells were lysed; the cell  
1643 lysates were incubated with Ni-NTA beads for 1.5 hr at 4°C in the presence of the  
1644 DMSO control, 10 μM BMS-806 or 10 μg/mL sCD4. Total cell lysates (Input) and  
1645 proteins bound to the Ni-NTA beads were Western blotted with a goat anti-gp120  
1646 antibody (upper panels) or the 4E10 anti-gp41 antibody (lower panels). (B) 293T cells  
1647 were transfected with plasmids encoding the indicated Envs, HIV-1 packaging proteins  
1648 and Tat, and a luciferase-expressing HIV-1 vector. Forty-eight hours later, cell  
1649 supernatants were filtered (0.45 μm) and incubated with different antibodies for 1 hr at  
1650 37°C before the mixture was added to Cf2Th target cells expressing CD4 and CCR5.

1651 Forty-eight hours after infection, the target cells were lysed, and the luciferase activity  
1652 was measured. The concentration of antibody required to inhibit 50% of virus infection  
1653 ( $IC_{50}$ ) was calculated using the GraphPad Prism program. (C) Filtered cell  
1654 supernatants containing recombinant viruses were incubated with sCD4 or the CD4-  
1655 mimetic compound BNM-III-170 for 1 hr at 37°C. Then the mixture was added to target  
1656 cells as described above. In the cold sensitivity assay, viruses were incubated on ice  
1657 for the indicated times, after which the virus infectivity was measured. The results  
1658 shown in A and C are representative of those obtained in at least two independent  
1659 experiments. The means and standard deviations derived from two independent  
1660 experiments or triplicate measurements are shown in B and C, respectively.

1661

1662 **Figure 3. Major contributions of the Q114E and Q567K changes to the respective**  
1663 **2-4 RED2 and 2-4 R phenotypes.** (A) The effects of the Q114E change on gp120-  
1664 trimer association (left panel) and virus sensitivity to cold, sCD4 and BNM-III-170 (right  
1665 panels) were measured as described in the legend to Figure 2. The sensitivities of  
1666 viruses with the wild-type HIV-1<sub>AD8</sub> Env and the 2-4 RED2 Env are shown for  
1667 comparison. (B) The effects of the Q567K change on gp120-trimer association (left  
1668 panel) and virus sensitivity to cold, sCD4 and BNM-III-170 (right panels) were  
1669 measured. The sensitivities of viruses with the wild-type HIV-1<sub>AD8</sub> Env and 2-4 R Env  
1670 are shown for comparison. The results shown are typical of those obtained in at least  
1671 two independent experiments. The right panels report the means and standard  
1672 deviations derived from triplicate measurements.

1673

1674 **Figure 4. Phenotypes of the E.2 and AE.2 Envs.** (A) HOS cells transiently  
1675 expressing His<sub>6</sub>-tagged Envs (wild-type HIV-1<sub>AD8</sub> Env, the E.2 Env, the AE.2 Env or the  
1676 HIV-1<sub>JR-FL</sub> Env) were lysed. Cell lysates were incubated with Ni-NTA beads for 1.5 hr at  
1677 4°C in the presence of the DMSO control or 10 µM BMS-806. Total cell lysates (Input)  
1678 and Ni-NTA-bound proteins were Western blotted with a goat anti-gp120 antibody  
1679 (upper panels) and the 4E10 anti-gp41 antibody (lower panels). (B) Recombinant  
1680 luciferase-expressing viruses with the indicated Envs were incubated with antibodies for  
1681 1 hr at 37°C, after which the mixture was added to Cf2Th-CD4/CCR5 target cells.  
1682 Forty-eight hours later, the target cells were lysed and the luciferase activity was  
1683 measured. The IC<sub>50</sub> values were calculated using the GraphPad Prism program. (C)  
1684 Recombinant luciferase-expressing viruses with the indicated Envs were incubated with  
1685 sCD4 or BNM-III-170 for 1 hr at 37°C before the mixture was added to Cf2Th-  
1686 CD4/CCR5 target cells. Cold sensitivity was assessed by incubation of the viruses on  
1687 ice for the indicated times, after which virus infectivity was measured on Cf2Th-  
1688 CD4/CCR5 cells as described above. The results are representative of those obtained  
1689 in at least two independent experiments. The values reported in B and C represent the  
1690 means and standard deviations from at least two independent experiments or triplicate  
1691 measurements, respectively.

1692

1693 **Figure 5. Correlations among key Env phenotypes.** The plot shows the relative  
1694 level of resistance to the CD4-mimetic compound BNM-III-170 versus the relative level  
1695 of cold resistance for the HIV-1 Env variants tested in this study. The levels of  
1696 resistance are scored as described in the legends to Tables 1-3: •, wild-type level; R,  
1697 resistant; S, sensitive. Key Env variants are designated with stars. Envs are colored

1698 according to their relative gp120-trimer association level, as measured by Ni-NTA  
1699 coprecipitation of gp120 with the His<sub>6</sub>-tagged gp41 glycoprotein: black, wild-type level;  
1700 gray, not determined or not applicable; light green, +; green, ++; red, -. The V255I  
1701 change is located near the binding site for CD4-mimetic compounds and may directly  
1702 affect Env interaction with BNM-III-170. Note that the E.2 and AE.2 Envs exhibit  
1703 resistance to cold and BNM-III-170 comparable to those of the HIV-1<sub>JR-FL</sub> and HIV-1<sub>BG505</sub>  
1704 Envs, but also display better gp160 processing and a tighter association of gp120 with  
1705 the Env trimer solubilized in detergent.

1706

1707 **Figure 6. Crosslinking of the wild-type HIV-1<sub>AD8</sub>, E.2 and AE.2 Envs.** (A) VLPs  
1708 consisting of the HIV-1 Gag-mCherry fusion protein and the wild-type HIV-1<sub>AD8</sub> Env, the  
1709 E.2 Env or the AE.2 Env were incubated with different concentrations of the DTSSP or  
1710 glutaraldehyde crosslinkers. After quenching the reactions, VLPs were pelleted and  
1711 lysed. The VLP proteins were analyzed by reducing or non-reducing PAGE,  
1712 respectively, followed by Western blotting. The ratio of gel-stable (dimers +  
1713 trimers):(gp120 + gp160) provides an indication of interprotomer crosslinking by  
1714 DTSSP. (B) Luciferase-expressing viruses pseudotyped with the wild-type HIV-1<sub>AD8</sub>,  
1715 E.2 or AE.2 Envs were incubated with the BS3 crosslinker. After quenching the  
1716 reaction, the viruses were added to Cf2Th-CD4/CCR5 cells. Luciferase activity in the  
1717 target cells was measured 48 hours later. The results shown in A and B are  
1718 representative of those obtained in at least two independent experiments. The values  
1719 reported in B represent the means and standard deviations derived from triplicate  
1720 measurements.

1721

1722 **Figure 7. Location of Env residues in a structural model of an HIV-1 Env trimer.**

1723 Env residues studied herein are depicted as CPK spheres in a PGT151-bound  
1724 HIV-1<sub>JR-FL</sub> Env ΔCT trimer (PDB: 5FUU) (82). The binding of two PGT151 Fabs  
1725 introduces asymmetry into the Env trimer. In this depiction, the PGT151 Fabs have  
1726 been removed from the structure. The individual Env protomers are colored pink, light  
1727 blue and gray. In this orientation, the gp120 subunits are at the bottom and gp41  
1728 subunits at the top of the figures. (A) Env residues (Gln 114 (magenta), Gln 567  
1729 (orange) and Ala 582 (blue)) associated with State 1-stabilizing changes are shown.  
1730 The distances between the C<sub>α</sub> atoms of Gln 114 and Gln 567 residues in this  
1731 asymmetric trimer structure are 11.6, 13.1 and 15.2 Å. The HR1<sub>N</sub> regions of the three  
1732 Env protomers differ in conformation. (B) Env residues (Lys 59, His 66, Gln 114, Gln  
1733 567 and Ala 582) associated with State 1-stabilizing changes are colored green. Env  
1734 residues (His 72, Thr 202, Gln 203, Arg 542, Ile 595, Leu 602 and Gln 658) associated  
1735 with State 1-destabilizing changes are colored red. Changes in the residues (Lys 117,  
1736 Lys 121 and Leu 587) colored yellow resulted in Envs that were resistant to cold and a  
1737 CD4-mimetic compound, but were subject to gp120 dissociation from the Env trimer  
1738 solubilized in detergent. The right panel shows the side-chain stacking of residues Gln  
1739 114, Lys 117 and Lys 121 near the Env trimer axis.

## Table 1

Env	Env Processing	Infectivity (%)	Resistance / Sensitivity compared to wild-type			gp120-trimer association
			Cold	sCD4	BNM-III-170	
Wild-type	•	•	•	•	•	•
Q114A	•	•	•	•	•	+
Q114D	+	•	RR	RR	RR	++
Q114E	+	+	RR	RR	RR	++
Q114K	No	ND	ND	ND	ND	NA
Q114N	•	ND	ND	ND	ND	•
Q114S	•	ND	ND	ND	ND	•
Q567A	•	+	•	•	•	•
Q567E	•	---	•	•	•	•
Q567K	+	•	R	R	R	++
Q567R	+	-	Slight R	•	•	+
Q114A Q567K	•	•	Slight R	R	R	++
Q114A Q567R	•	•	•	•	•	+
Q114D Q567R	+	•	R	RR	RR	++
Q114E Q567A	+	+	RR	RR	RR	++
Q114E Q567K	+	•	RRR	RRR	RRR	++
Q114E Q567E	+	-	R	•	R	++
Q114E Q567R	+	•	RR	RR	RR	++
Q114K Q567E	No	ND	ND	ND	ND	NA

**Table 2**

Env	Env Processing	Infectivity (%)	Resistance / Sensitivity compared to wild-type			gp120-trimer association
			Cold	sCD4	BNM-III-170	
Wild-type	•	•	•	•	•	•
Q114E	+	+	RR	RR	RR	++
Q567K	•	•	R	R	R	++
Q114E Q567K	+	•	RRR	RRR	RRR	++
H72A	--	---	R	•	•	NA
H72K	--	---	•	SS	SS	NA
H72Q	--	---	•	ND	SS	NA
H72A Q114E	-	--	R	•	RR	-
H72K Q114E	-	---	•	S	SS	-
H72Q Q114E	-	-	R	S	•	-
T202K	•	-	SS	S	SS	•
T202R	•	-	SS	S	SS	•
T202A	•	-	SSS	SSS	SSS	-
T202Q	•	•	SSS	SSS	SSS	-
Q114E T202K	+	+	SS	S	SS	+
Q114E T202R	+	+	SS	S	SS	+
Q114E T202A	•	•	SSS	SS	SSS	•
Q114E T202Q	•	+	SSS	SS	SSS	•
Q203A	•	•	SS	ND	SSS	-
Q114E Q203A	+	•	•	ND	•	•
K117A	•	•	RR	ND	RR	•
K117Q	ND	-	R	ND	RR	ND
K121A	•	--	•	ND	RR	-
K121Q	ND	-	R	ND	RR	ND
Q114E K117A	•	•	RR	ND	RR	•
Q114E K121A	+	-	Slight R	ND	RR	+
H66N	•	-	R	RRR	RRR	•
A582T	•	•	RRR	RR	RR	+
L587A	-	•	RR	R	RR	-
Q114E H66N	+	•	RR	RRR	RRR	++
Q114E A582T	+	•	RRR	RR	RRR	++
Q567K A582T	•	•	RRR	RR	RRR	+
Q114E L587A	+	•	RR	RR	RR	•
Q114E Q567K A582T	+	+	RRRR	RRRR	RRRR	++
Q114E Q567K L587A	+	-	RR	RR	RRR	+

**Table 3**

Env	Env Processing	Infectivity (%)	Resistance / Sensitivity compared to wild-type			gp120-trimer association
			Cold	sCD4	BNM-III-170	
Wild-type	•	•	•	•	•	•
E.2	+	+	RRR	RRR	RRR	++
AE.2	+	-	RRRR	RRRR	RRRR	++
E.2 K117A	+	•	RRR	RRR	RRR	-
AE.2 K117A	+	--	RRRR	RRRR	RRRR	+
K59A	•	•	R	R	RR	•
V255I	•	•	RR	NA*	NA*	•
E.2 K59A	+	-	RRR	RRR	RRR	++
AE.2 K59A	+	--	RRRR	RRRR	RRRR	++
E.2 K59A V255I	+	---	RRRR	NA*	NA*	++
E.2 V255I	+	-	RRRR	NA*	NA*	++
AE.2 V255I	+	---	RRRR	NA*	NA*	++
AE.2 K59A V255I	+	---	RRRR	NA*	NA*	++
K59A Q114E V255I	+	--	RRRR	NA*	NA*	++
R542V	-	---	S	SSS	SSS	-
I595F	-	-	R	SSS	SSS	-
L602H	-	-	S	SSS	SSS	-
2-4 RM6 AE	+	-	RRR	RRR	RRR	++
2-4 RM6 AE R542V	+	---	RR	RRR	RR	++
2-4 RM6 AE I595F	+	---	R	•	•	++
2-4 RM6 AE L602H	+	--	RRR	RRR	RR	++

# Figure 1

**A**

## Lysine Polymorphisms

## Acidic Polymorphisms

gp41 and gp120 C-terminus	Set 1	Set 4	Set 6	ED2
	R557K R633K Q658K N677K	R557K R633K Q658K N677K Q567K	R557K R633K Q658K N677K Q567K E492K	N92E Q114E S164E S275E Q507E M621E G640D
gp120 trimer-association domain	Set 2	Set 5	Set 7	R
	R166K R178K R419K	R166K R178K R419K T202K	R166K R178K R419K T202K Q328K	R315K
gp120 inner domain	Set 3			
	T49K T63K V65K			

**B**

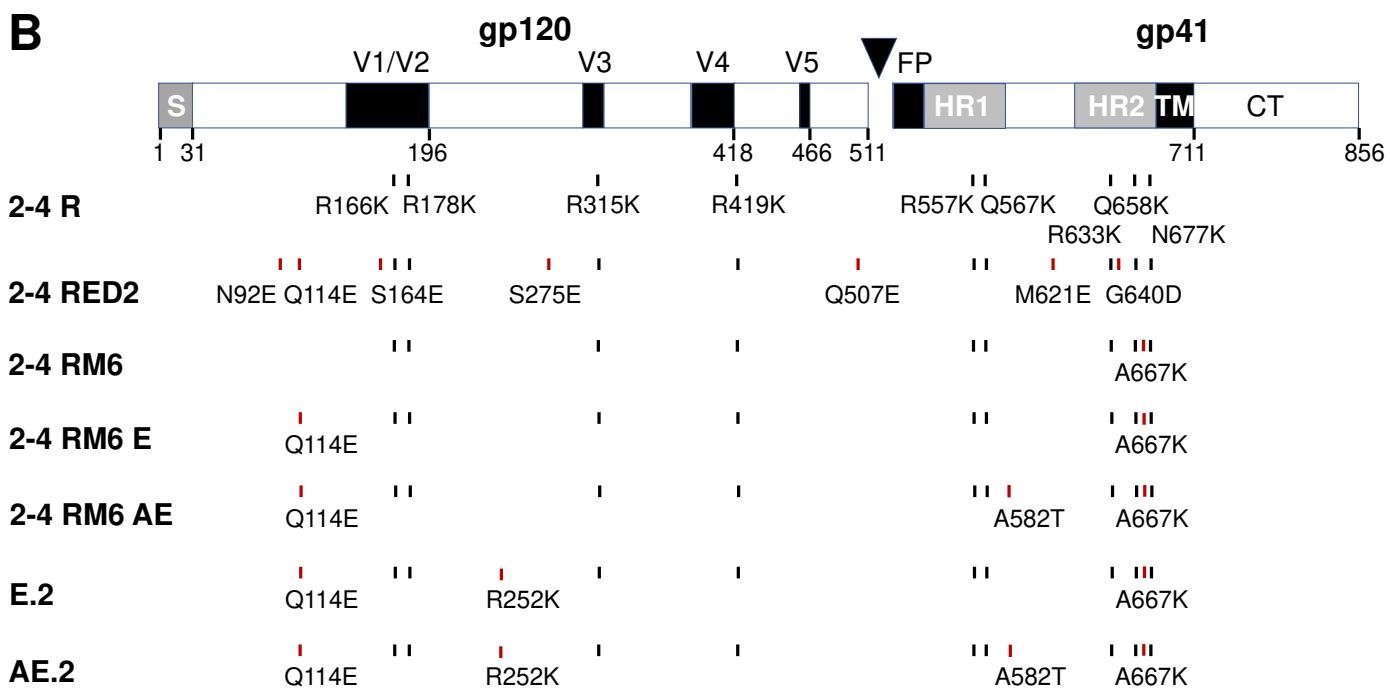


## Figure 2

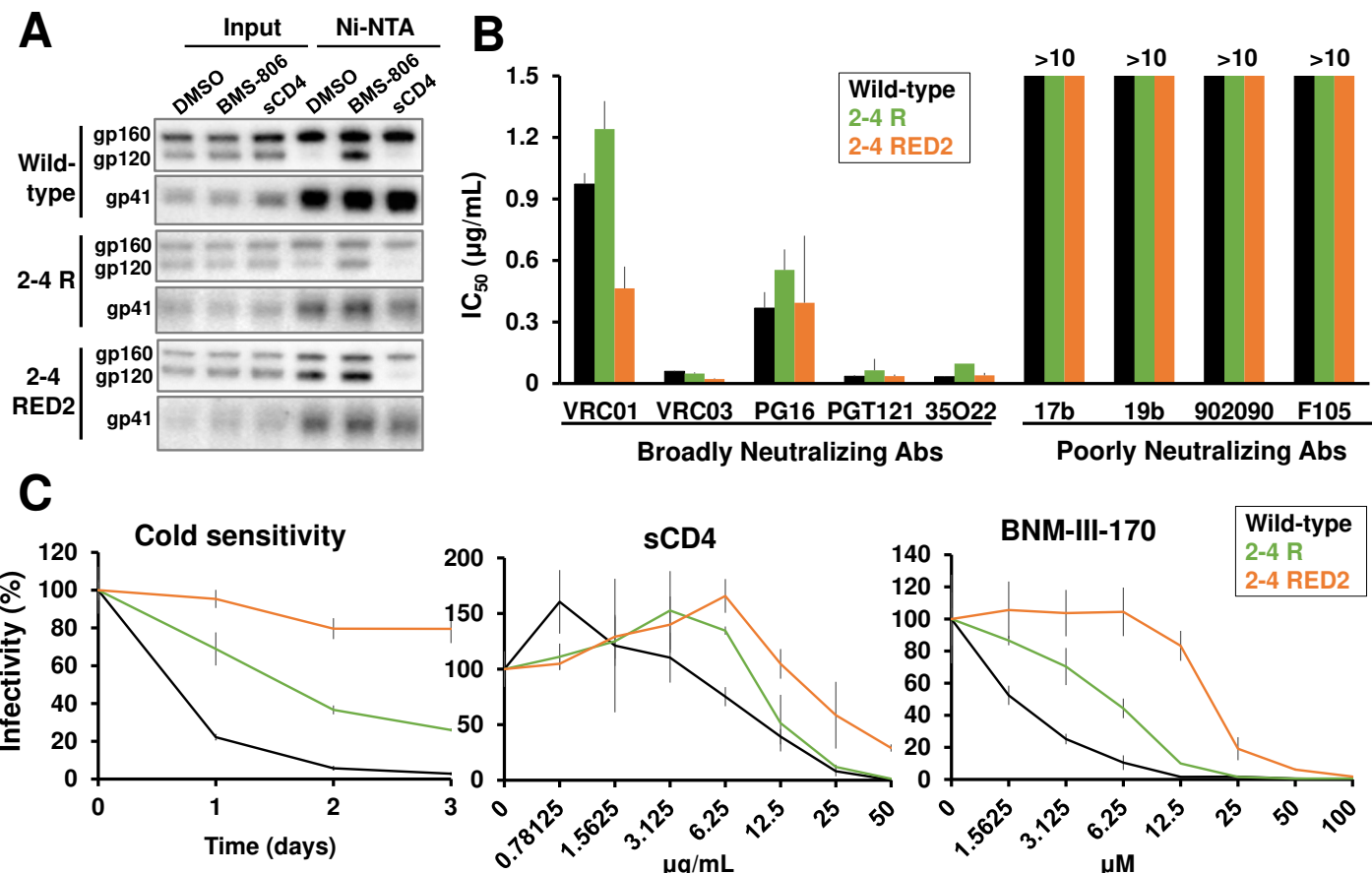
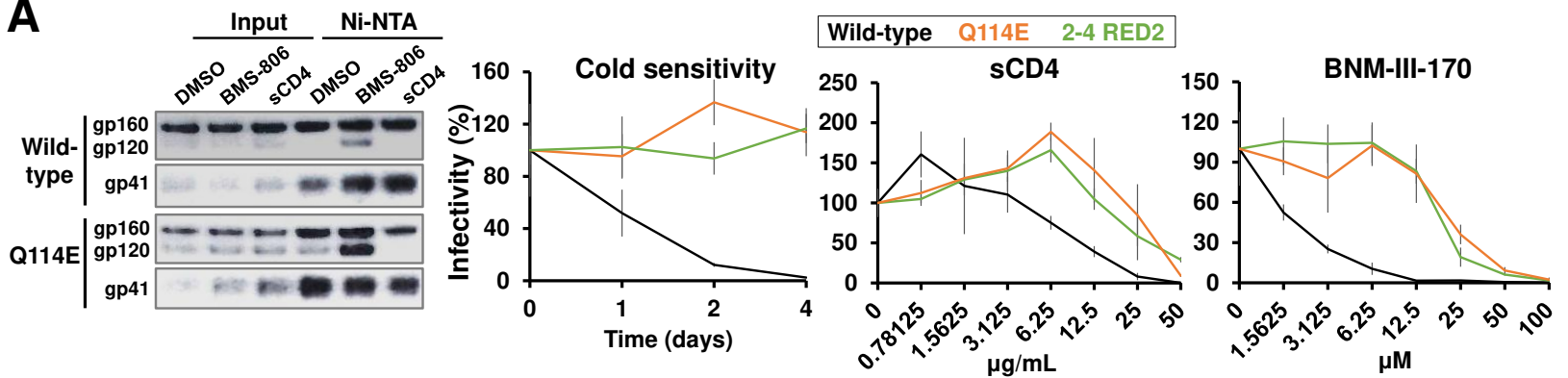


## Figure 3

**A**



**B**

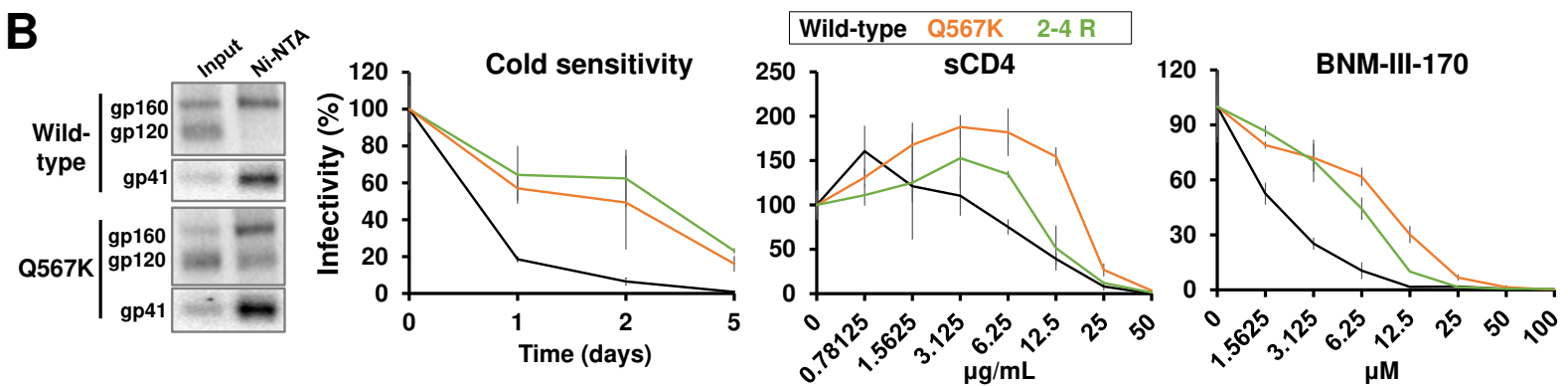
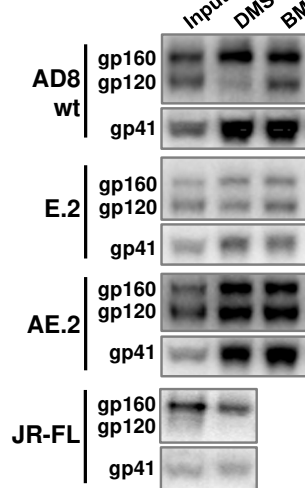
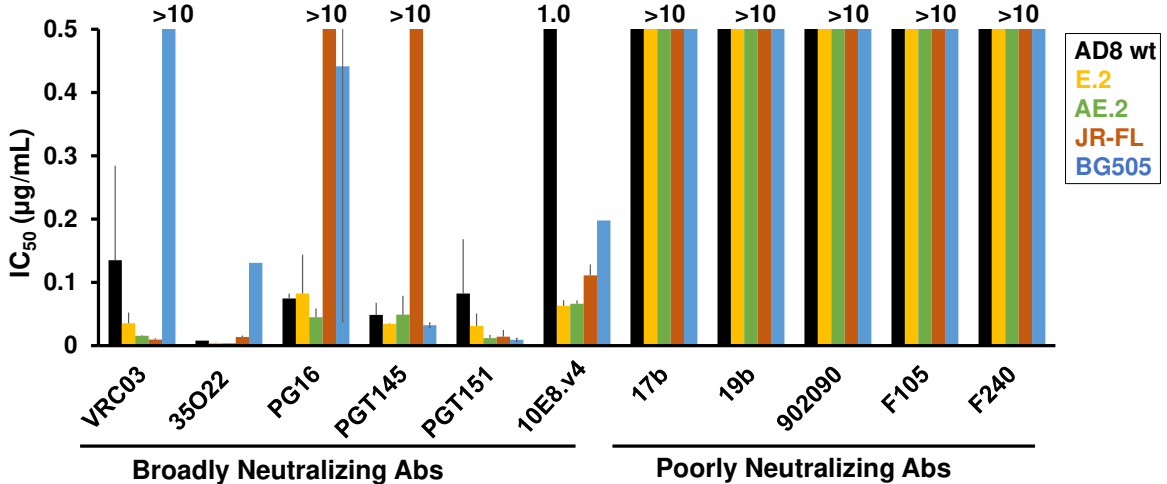


## Figure 4

**A**



**B**



**C**

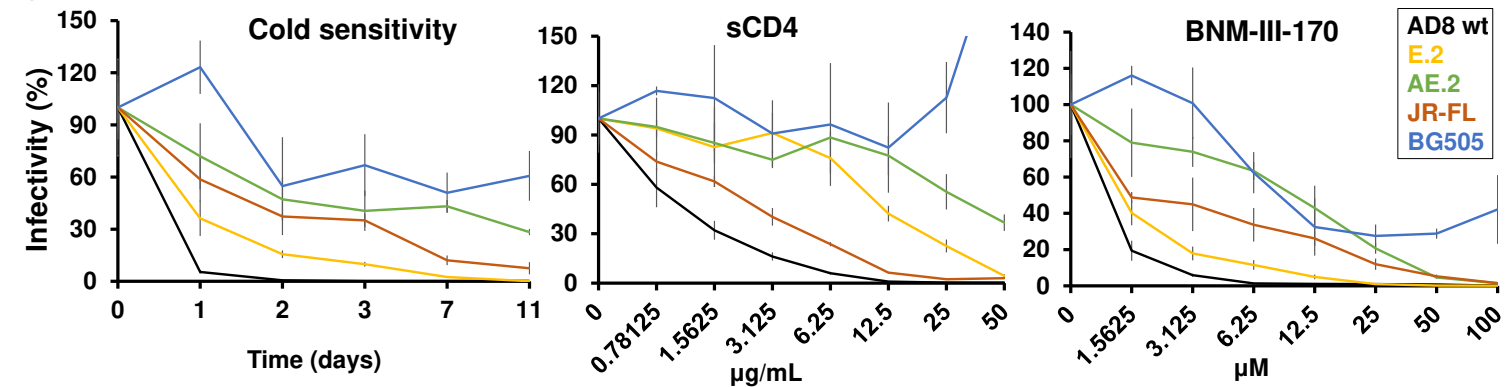


## Figure 5

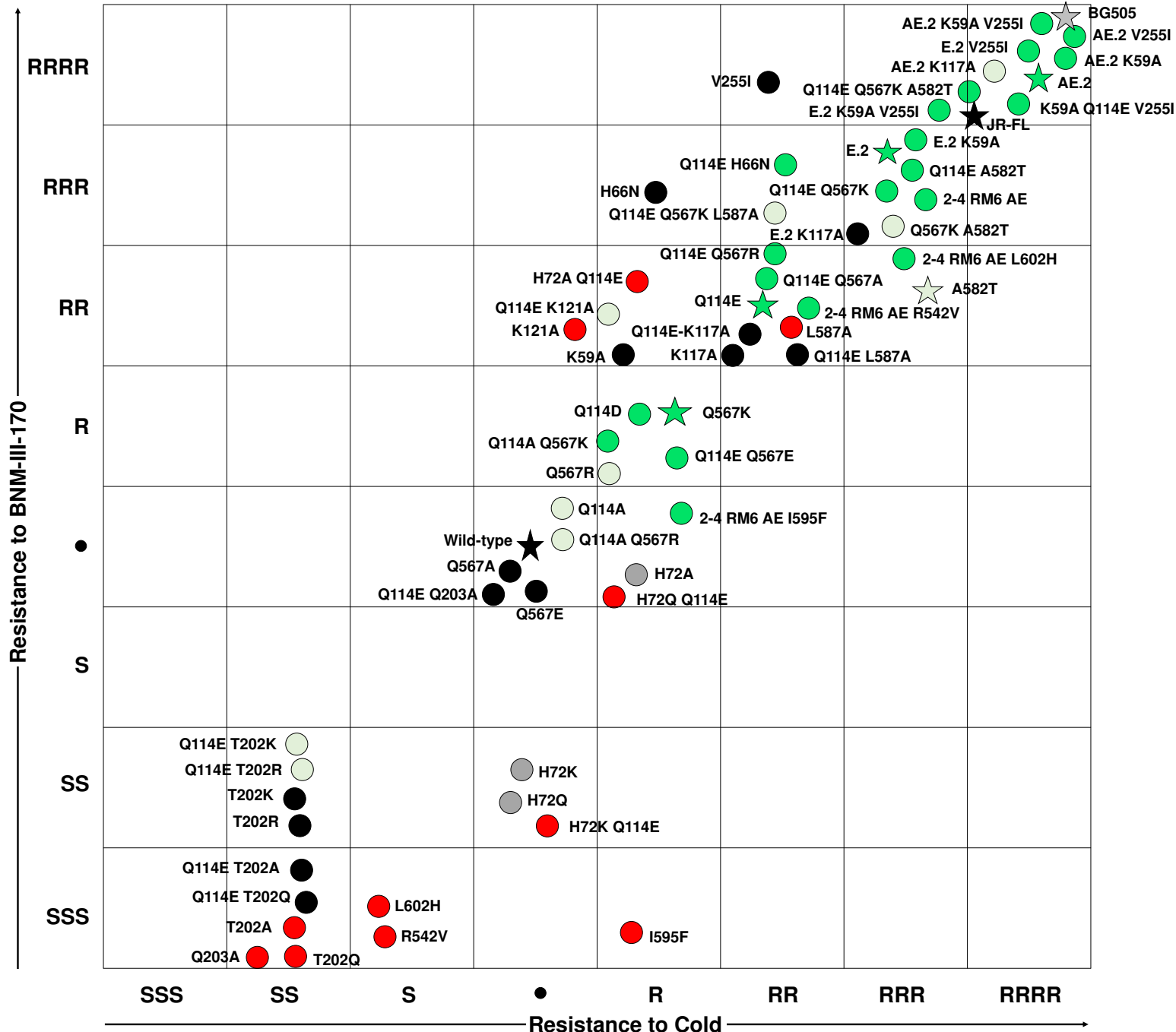


## Figure 6

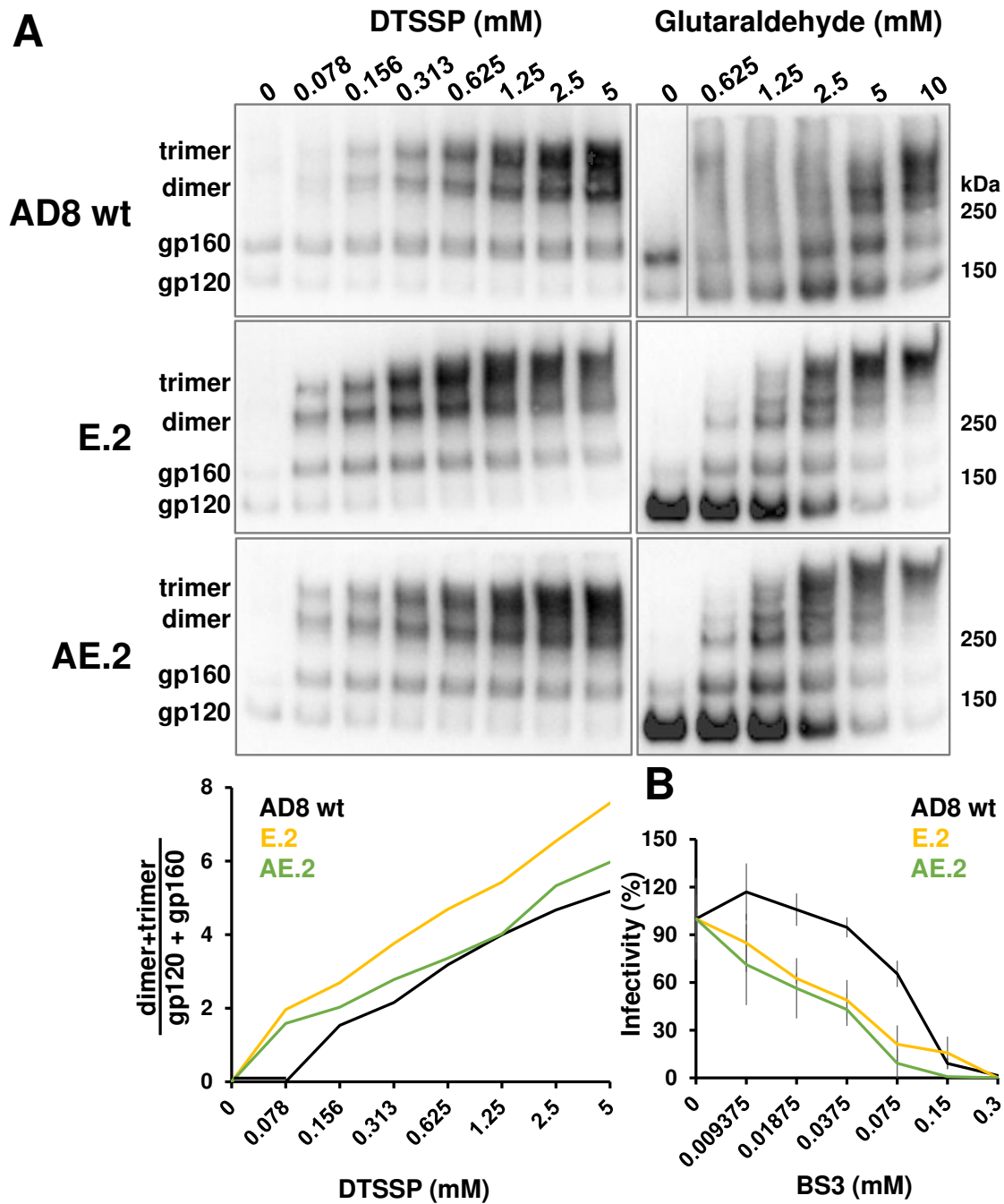


**Figure 7**

